UNIVERSIDADE DE SÃO PAULO
FACULDADE DE ODONTOLOGIA DE BAURU

CAMILA CORREA DA SILVA BRAGA DE MELO

Mineral-induced bubbling effect and biomineralization as strategies to create highly porous and bioactive scaffolds for dentin tissue engineering

Bubbling effect induzido por mineral e biomineralização como estratégias para criar scaffolds altamente porosos e bioativos para engenharia tecidual dentinária

BAURU
2021

CAMILA CORREA DA SILVA BRAGA DE MELO

Mineral-induced bubbling effect and biomineralization as strategies to create highly porous and bioactive scaffolds for dentin tissue engineering

Bubbling effect induzido por mineral e biomineralização como estratégias para criar scaffolds altamente porosos e bioativos para engenharia tecidual dentinária

Dissertação constituída por artigo apresentada à Faculdade de Odontologia de Bauru da Universidade de São Paulo para obtenção do título de Mestre em Ciências no Programa de Ciências Odontológicas Aplicadas, na área de concentração Dentística.

Orientadora: Profa. Dra. Diana Gabriela Soares dos Passos

BAURU
2021

Correa da Silva Braga de Melo, Camila
Mineral-induced bubbling effect and biomineralization as strategies to create highly porous and bioactive scaffolds for dentin tissue engineering / Camila Correa da Silva Braga de Melo. -- Bauru, 2021.

69 p. : il. ; 31 cm.

Dissertação (mestrado) -- Faculdade de Odontologia de Bauru, Universidade de São Paulo, 2021

Orientadora: Profa. Dra. Diana Gabriela Soares dos Passos

Autorizo, exclusivamente para fins acadêmicos e científicos, a reprodução total ou parcial desta dissertação/tese, por processos fotocopiadores e outros meios eletrônicos.

Assinatura:

Data:

Comitê de Ética da FOB-USP
Protocolo nº:
Data:

ERRATA

Universidade de São Paulo
Faculdade de Odontologia de Bauru

Assistência Técnica Acadêmica
Serviço de Pós-Graduação

FOLHA DE APROVAÇÃO

Dissertação apresentada e defendida por
CAMILA CORREA DA SILVA BRAGA DE MELO
e aprovada pela Comissão Julgadora
em 08 de dezembro de 2021.

Prof.ª Dr.ª **ANDRÉA CANDIDO DOS REIS**
FORP

Prof.ª Dr.ª **JOSIMERI HEBLING COSTA**
FO-UNESP

Prof.ª Dr.ª **FLAVIANA BOMBARDA DE ANDRADE**
FOB-USP

Prof.ª Dr.ª **DIANA GABRIELA SOARES DOS PASSOS**
Presidente da Banca
FOB - USP

Izabel Regina Fischer Rubira Bullen

Profª. Drª. **Izabel Regina Fischer Rubira de Bullen**
Presidente da Comissão de Pós-Graduação

Al. Dr. Octávio Pinheiro Brisolla, 9-75 – Bauru-SP – CEP 17012-901 – C.P. 73
e-mail: posgrad@fob.usp.br – Fone/Fax (0xx14) 3235-8223
http://www.fob.usp.br

DEDICATÓRIA

Dedico esse trabalho aos meus pais, ***Glória*** e ***Benedito***, por todo amor, dedicação e incentivo, sempre me ensinando que nosso conhecimento não pode ser tirado de nós e que ele é capaz de mudar as nossas vidas.

AGRADECIMENTOS GERAIS

À **Deus** por ser consolo e abrigo nos momentos mais difíceis e por mostrar que com Amor tudo é possível.

Aos meus pais, **Glória** e **Benedito**. À minha mãe, por sempre ter palavras de ânimo e incentivo, e ao meu pai que, mesmo não estando mais presente fisicamente, se faz presente em meu coração e me lembra todos os dias que devemos sorrir mesmo em meio às dificuldades. Se hoje eu tenho a oportunidade de sonhar, meus pais tiveram mais que sonhar. Lutaram e batalharam muito por mim antes mesmo de eu nascer. Meu caminho tem sido mais fácil porque eles trilharam caminhos desafiadores. Serei eternamente grata e farei de tudo para honrar tamanho sacrifício.

Ao meu irmão **Henrique** por sempre me apoiar e incentivar a estudar. Obrigada por todas as conversas. Diante da vastidão do tempo e da imensidão do universo, é um imenso prazer para mim dividir um planeta e uma época com você.

Ao meu companheiro **Carlos**, por estar sempre presente e me ouvir falar o tempo todo sobre a pesquisa. Você me trouxe paz nesse período.

À minha família do coração. **Patrícia e Ruben**, serei eternamente grata por sempre me receberem tão bem, com carinho e cuidado, me tratando como filha.

Aos amigos **Adrielle, Caren, Érika Viruel, Jéssica, Laís Reis, Leonardo, Marcela, Mariana, Mariele, Orlando, Rafaela, Victor, Vitória e Vítor Abner** por todo carinho e apoio.

À minha orientadora **Profa. Dra. Diana Gabriela Soares dos Passos** por confiar no meu trabalho, sempre me incentivando e servindo de exemplo de competência, compromisso e dedicação. Nossas conversas sempre me inspiram, tanto pessoal quanto profissionalmente. É maravilhoso poder contar com alguém que está sempre disposta a ajudar e que nos incentiva a sermos melhores. Sinto-me privilegiada por ser sua orientada.

Aos meus colegas do **Laboratório de Cultura de Células e Engenharia Tecidual – LACET**, **Larissa, Fernanda, Érika, Ester, Leandro, Vitor, Marjorie, Andressa, Marlene e Glória**. Ter pessoas como vocês no ambiente de trabalho faz tudo ser mais leve. Obrigada por toda ajuda, trocas e por sempre serem tão solícitos.

Aos meus colegas de mestrado **Ana Carolina, Constantino, Denner, Larissa Ikejiri, Laís, Marta, Paulo, Pedro e Vanessa.** Sou grata por todas as trocas que tivemos nesse período. Obrigada por toda ajuda e por tornarem o mestrado mais leve. Mesmo em um período tão conturbado desenvolveram trabalhos excelentes. Tenho muito orgulho de vocês.

Aos funcionários do **Departamento de Dentística**, por serem tão competentes, dedicados e atenciosos. O trabalho de vocês é fundamental para a qualidade desse programa de Mestrado.

Aos professores **Ana Flávia Sanches Borges, Adilson Yoshio Furuse, Juliana Fraga Soares Bombonatti, Rafael Mondelli, Linda Wang e Sérgio Ishikiriama**, por todos os ensinamento desde a época da graduação.

Aos colegas veteranos de mestrado **Genine, Alyssa, Daniella, Naoki, Juliana e Fernanda Sandes** por toda ajuda e troca de experiências.

AGRADECIMENTOS INSTITUCIONAIS

À **Faculdade de Odontologia de Bauru – Universidade de São Paulo (FOB/USP),** por fornecer toda a infraestrutura necessária para a realização desse trabalho.

À **Coordenação de Aperfeiçoamento de Pessoal de Nível Superior (CAPES)** – Codigo de Financiamento 001, que financiou parte deste estudo.

À **FAPESP (Fundação de Amparo à Pesquisa do Estado de São Paulo)** que através do processo n° 2019/06884-4, vinculado ao Programa Jovens Pesquisadores em Centros Emergentes (processo nº 2016/15674-5), financiou e permitiu o desenvolvimento desta pesquisa.

“Tudo posso naquele que me fortalece”

Filipenses 4:13

ABSTRACT

Mineral-induced bubbling effect and biomineralization as strategies to create highly porous and bioactive scaffolds for dentin tissue engineering

The objective of this study was to develop porous chitosan (CH) scaffolds containing different mineral phases, based on a ‘bubbling effect’ technique and subjected to a biomineralization protocol, to create biomimetic strategies to improve the odontogenic potential of human dental pulp cells (HDPCs). Suspensions containing the mineral phases calcium hydroxide (Ca), nanohydroxyapatite (nHA), and β-tricalcium phosphate (βTCP) were added to the CH solution at a 1:2 (v/v) ratio. The scaffolds were synthesized by a phase-separation technique and biomineralized by incubation in Simulated Body Fluid (SBF) for 5 days at 37°C and under constant stirring. The samples were characterized as to their morphology, chemical composition, degree of degradability, and calcium-release capacity. The biological behavior of the HDPCs in direct and indirect contact with the scaffolds was analyzed by cell viability (Live/Dead® and Alamar Blue) and odontogenic differentiation (ALP activity and Alizarin Red) assays. The addition of mineral phases to CH led to the appearance of larger pores and higher degrees of porosity, with complexation of calcium and phosphate ions to the chitosan structure. CH-Ca and CH-nHA pores were round, well-distributed, and with an interconnected network, whereas other formulations had more disorganized architecture. Incubation in SBF was responsible for disorganization of the porous structure, except for CH-Ca formulation. A disperse and slightly mineral-like deposition was detected on CH and CH-Ca scaffolds subjected to SBF treatment, whereas large mineral deposits were observed on CH-nHA and CH-βTCP. The deposition of calcium phosphate by SBF, indicative of hydroxyapatite, was confirmed chemically by FTIR. The mineral-containing scaffolds, incubated or not in SBF, featured a controlled degradation profile, whereas plain CH formulations were stable throughout 28 days of incubation in phosphate-buffered saline solution. The CH-βTCP and CH-nHA showed continuous Ca^{2+} release, whereas CH-Ca released less Ca^{2+}, with a peak at 7 days. A similar trend was detected for SBF-treated counterparts. The cells seeded onto the scaffolds remained viable at all time-points. The porous and interconnected porous architecture of CH-Ca, CH-nHA, and

CH-Ca-SBF allowed cells to infiltrate and spread throughout the scaffold structure, whereas in other formulations cells were dispersed or agglomerated. There was an increase in cell viability in the groups containing mineral phases and biomineralized compared with the control (CH), which was more evident for SBF-treated samples. There was also an increase in odontogenic differentiation and mineralized matrix deposition in these groups compared with the groups without biomineralization, in both experimental models. A significant increase in mineralized matrix deposition (by 8.4 to 18.9 times) was observed for CH-Ca-SBF, CH-nHA-SBF, and CH-βTCP-SBF in comparison with plain CH. Therefore, biomineralization of chitosan scaffolds containing different mineral phases was responsible for increasing the capacity of mineralized matrix deposition by pulpal cells, with potential for use in dentin tissue engineering.

Key words: scaffold, chitosan, mineral, biomineralization, dentin, vital pulp therapy, HDPC

RESUMO

Bubbling effect induzido por mineral e biomineralização como estratégias para criar scaffolds altamente porosos e bioativos para engenharia tecidual dentinária

O objetivo desse estudo foi desenvolver scaffolds porosos de chitosana (CH) contendo diferentes fases minerais, baseados na técnica “bubbling effect” e submetidos a um protocolo de biomineralização, para criar estratégias biomiméticas para melhorar o potencial odontogênico das células da polpa dentária humana (HDPCs). Suspensões contendo as fases minerais hidróxido de cálcio (Ca), nanohidroxiapatita (nHA) e β-Fosfato Tricálcico (βTCP) foram adicionadas à solução de CH em uma proporção de 1:2 (v/v). Os scaffolds foram sintetizados pela técnica de separação de fases e biomineralização através da incubação em Simulated Body Fluid (SBF) por 5 dias a 37ºC e sob agitação constante. As amostras foram caracterizadas de acordo com a morfologia, composição química, grau de degradabilidade e capacidade de liberação de cálcio. O comportamento biológico das HDPCs em contato direto e indireto com os scaffolds foi analisado através dos ensaios de viabilidade celular (Live/Dead® e Alamar Blue) e diferenciação odontogênica (atividade de ALP e Alizarin Red). A adição de fases minerais à CH levou ao aparecimento de poros maiores e maiores graus de porosidade, com a complexação de íons cálcio e fosfato à estrutura da quitosana. Os poros dos grupos CH-Ca e CH-nHA apresentaram-se redondos, bem distribuídos e com uma rede de poros interconectada. A incubação em SBF foi responsável pela desorganização da estrutura porosa, exceto para a formulação CH-Ca. Deposição dispersa e discreta, semelhante a mineral, foi detectada nos scaffolds de CH e CH-Ca submetidos ao tratamento com SBF, enquanto que maiores depósitos minerais foram observados em CH-nHA e CH-βTCP. A deposição de fosfato de cálcio pelo SBF, indicativa de hidroxiapatita, foi confirmada quimicamente pelo FTIR. Os scaffolds contendo fases minerais, incubados ou não em SBF, apresentaram um perfil de degradação controlado, enquanto as formulações com CH pura foram estáveis ao longo dos 28 dias de incubação em PBS. CH-βTCP e CH-nHA apresentaram liberação contínua de Ca^{2+}, enquanto que CH-Ca apresentou menor liberação, com pico aos 7 dias. Uma tendência semelhante foi detectada para as contrapartes tratadas com SBF. As células semeadas sobre os scaffolds permaneceram viáveis em todos os períodos de análise. A arquitetura porosa e interconectada dos grupos CH-Ca, CH-nHA e CH-Ca-SBF permitiu que as células infiltrassem e espalhassem através da estrutura do scaffold, enquanto que nas outras formulações as células apresentaram-se dispersas ou aglomeradas. Houve um aumento na viabilidade celular nos grupos contendo fases minerais e biomineralizados comparados ao controle (CH), que foi mais evidente nas amostras tratadas em SBF. Também houve um aumento na diferenciação odontogênica e na deposição de matriz mineralizada nesses grupos comparados aos grupos sem biomineralização, em ambos os modelos experimentais. Um significativo aumento na deposição de matriz mineralizada (de 8.4 a 18.9 vezes) foi observado para CH-Ca-SBF, CH-nHA-SBF e CH- βTCP-SBF em comparação à CH pura. Portanto, a biomineralização de scaffolds de quitosana contendo diferentes fases minerais foi responsável por aumentar a capacidade de deposição de matriz mineralizada por células pulpares, com potencial para uso em engenharia tecidual dentinária.

Palavras-chave: scaffold, quitosana, mineral, biomineralização, dentina, terapia da polpa vital, HDPC

TABLE OF CONTENTS

1 INTRODUCTION 15

2 ARTICLE 21

3 FINAL CONSIDERATIONS 57

REFERENCES 61

APPENDIX 69

1 INTRODUCTION

1 INTRODUCTION

Tissue engineering concepts have enjoyed wide application in contemporary medicine and dentistry. This research field is based on a solid multidisciplinary approach by integrating principles of materials science, pharmacology, and cellular and molecular biology, to solve clinical problems more effectively. This dynamic is supported by the interaction of three pillars: a biomaterial that acts as a temporary substitute for extracellular matrix (scaffold), precursor cells with regenerative potential, and biological factors for modulating cellular responses. [1, 2, 3, 4]

Therapeutic strategies related to tissue engineering can be categorized into three classes: conductive, where scaffolds are used in a passive way to facilitate the growth of existing tissues; inductive, involving the activation of cells in tissues surrounding the biomaterial implantation site via stimulation of specific biological signals; and cell transplantation, in which the seeding of cells on scaffolds is performed in the laboratory, followed by their cultivation in a specific differentiation medium, for induction of the desired cell phenotype and implantation of the construct in the surgical site. [5] Cell induction therapy has been gaining increasing popularity among researchers due to the absence of ethics issues, since this therapy does not involve the implantation of stem cells into humans, resulting in lower operational costs and higher technical practicality, thus uniting laboratory experimentation with clinical applicability. Since this type of strategy involves the modulation of tissue regeneration by host cells, it has been called *cell homing.* [6, 7, 8]

The cell homing strategy has been the focus of studies in regenerative dentistry, specifically by the development of materials with the ability to induce dentin repair/regeneration through the activation of the reparative dentinogenesis process from pulpal and periapical stem cells. Scaffolds play a crucial role in this process, since they serve as a framework for the tissue deposition process. Moreover, they must modulate the chemotaxis events of resident cells to their structure, followed by their adhesion, spreading, infiltration, proliferation, cell differentiation, and stimulation of secretory activity. [6, 7, 8] In this sense, biomaterials with a composition similar to that of dentin have been proposed as an alternative to direct pulp-capping, based on the fact that they can act as an artificial extracellular matrix, serving as physical support and a temporary model for initial cell attachment, benefiting the repair of this tissue. [9, 10, 11, 12]

Chitosan (CH) has been widely used as a biomaterial in the formulation of scaffolds for tissue regeneration due to its biodegradability, biocompatibility, low cost, and easy manipulation. [13, 14, 15] Its chemical structure is similar to that of glycosaminoglycans, which allows for interactions with tissue glycosaminoglycans and proteoglycans, facilitating its integration into the body after implantation. In addition, this chemical structure favors cell adhesion and proliferation in chitosan scaffolds, as well as allowing for several possibilities of covalent and ionic modifications, favoring an adjustment of mechanical and biological properties when combined with other materials. [16] The literature demonstrates that chitosan is cytocompatible and bioactive with pulpal cells, allowing for adequate cell interaction and inducing the processes of chemotaxis and mineralized matrix deposition in vitro and in vivo. [17, 8]

In addition to chemical composition, the three-dimensional (3D) architecture of scaffolds is critical to the repair process. Thus, scaffolds with a high degree of porosity and structures with interconnected pores are essential for favoring regeneration. [10, 18] Chitosan solutions can be easily processed into porous scaffolds by crystallization of the solvent at low temperatures (from -20 to -1980°C), followed by freeze-drying. Although widely used, this technique does not provide adequate control of pore size and interconnectivity. [16, 19] These characteristics can be controlled through the use of porogens, which act as a mold in which the polymer is infiltrated and subjected to the phase-separation process. Then, the porogen is leached out, and the polymer is subjected to lyophilization. This process can be produced by the use of sugar, paraffin, or sodium chloride crystals, with predetermined sizes and shapes. [20]

A technique developed by the researchers involved in this project facilitated the creation of an ordered and interconnected macro-pore network in chitosan scaffolds, containing calcium complexed to its structure. For this process, a suspension of calcium hydroxide [$Ca(OH)_2$] was incorporated into the chitosan solution in acetic acid ($2CH_3COOH$), resulting in the formation of calcium acetate [$Ca\ (CH_3COO^-)_2$], the latter releasing calcium carbonate ($CaCO_3$). In the presence of $2CH_3COOH$, $CaCO_3$ releases carbon dioxide (CO_2). The release of CO_2 during the slow and gradual freezing process allows for the creation of bubbles that undergo expansion within the polymeric mesh, creating interconnected pores containing calcium in their structure, thus called chitosan-calcium scaffolds (CH-Ca). This technique has been named the *mineral-induced bubbling effect*. Both the pore diameter and the total porosity of the material were increased compared with those of pure chitosan scaffolds. Fourier-Transform Infrared Spectroscopy (FTIR) analysis demonstrated the incorporation of calcium into the chemical structure of chitosan, as well as showing that it was possible to modulate the degree of degradability through the establishment of cross-linking, to obtain a material with controlled degradability, allowing new tissue to develop. In addition, the CH-Ca scaffold acted as a calcium-release system capable of increasing the odontogenic potential of human dental pulp cells, therefore increasing the deposition of mineralized tissue. [21]

Surface morphology should also be taken into consideration because it will exert a direct impact on cell adhesion, proliferation, and differentiation. An increase in the capacity for mineralized tissue deposition has already been demonstrated when mesenchymal stem cells adhere to surfaces with nano-topography compared with smooth surfaces. [22, 20] Based on this, hydroxyapatite (HA) [$Ca_{10}(PO_4)_6(OH)_2$], an important calcium phosphate of biological interest, has been tested as a compositional and surface modifier in scaffolds. This addition can improve the uniformity of osteoblastic cell spreading and bone tissue formation when compared with non-combined materials, because the similarity to a bone/dentin extracellular matrix leads to enhanced interaction with precursor cells, as well as increasing the expression of some important bone markers, such as osteocalcin and bone sialoprotein, and improving the mechanical strength of scaffolds. [9, 23, 13, 24, 25, 26, 21]

In this context, other calcium phosphates have been extensively studied as biomaterials for presenting favorable characteristics such as biocompatibility, bioactivity, the absence of toxicity, variable degradation rates, and osteoconductivity. [27] Among these, β-tricalcium phosphate (βTCP) [$Ca_3(PO_4)_2$] is currently among the most-used in bone regeneration, because it presents a moderate degradation rate, is osteoconductive and bioactive, has a calcium and phosphate ratio similar to that of natural bone, and increases the differentiation and proliferation of mesenchymal stem cells. For this reason, scaffolds containing βTCP have been investigated in tissue engineering, and their application has also been suggested for targeting odontogenic differentiation. [28, 29, 30, 31, 32]

Calcium phosphates can also be applied to coat materials, generating a conductive surface that would favor tissue formation and growth. [27] Incubation of scaffolds in Simulated Body Fluid (SBF), a solution with composition, pH, temperature, and ionic concentration similar to those of human blood plasma, has been used as a biomineralization technique to modify the surfaces of scaffolds through the deposition of partially carbonated hydroxyapatite, mimicking the biological process of bone and tooth formation. [33] This biomimetic approach aims to modify the internal pore wall without changing the structure and properties of the scaffolds. [9, 10] In this sense, this process can be used as a simple surface-modification technique for scaffolds used in bone and dentin repair and regeneration. [34, 9]

Thus, based on this literature overview, a hypothesis arises that incorporating mineral phases containing calcium-phosphate into chitosan during scaffold formulation following the fabrication process established by our group [21] would also promote the mineral-induced bubbling effect, creating novel formulations with bioactive potential greater than that of calcium hydroxide. Also, associating these formulations to a biomineralization procedure in SBF would improve the odontogenic potential of pulp cells in contact with scaffold surfaces, due to the increased similarity to native mineralized tissues. Therefore, in this work, the mineral-induced bubbling effect and SBF biomineralization techniques were performed to create biomimetic chitosan scaffolds for application in dentin tissue engineering, with bioactive potential being evaluated by in vitro cell culture methods.

2 ARTICLE

2 ARTICLE

The article presented in this Dissertation was written according to the Journal of Biomedical Materials Research Part B: Applied Biomaterials instructions and guidelines for article submission.

Mineral-induced bubbling effect and biomineralization as strategies to create highly porous and bioactive scaffolds for dentin tissue engineering

Camila Correa da Silva Braga de Melo

DDS, MS student, Department of Operative Dentistry, Endodontics and Dental Materials, Sao Paulo University – USP, Bauru School of Dentistry, Bauru, SP, Brazil. Al. Dr. Octavio Pinheiro Brizola, 9-75, Bauru, SP, Brazil. Postal code: 17012-901.

Fernanda Balestrero Cassiano

DDS, PhD student, Department of Operative Dentistry, Endodontics and Dental Materials, Sao Paulo University – USP, Bauru School of Dentistry, Bauru, SP, Brazil. Al. Dr. Octavio Pinheiro Brizola, 9-75, Bauru, SP, Brazil. Postal code: 17012-901.

Érika Soares Bronze-Uhle

DDS, PhD Department of Operative Dentistry, Endodontics and Dental Materials, Sao Paulo University – USP, Bauru School of Dentistry, Bauru, SP, Brazil. Al. Dr. Octavio Pinheiro Brizola, 9-75, Bauru, SP, Brazil. Postal code: 17012-901.

Vitor de Toledo Stuani

DDS, MS, PhD Department of Operative Dentistry, Endodontics and Dental Materials, Sao Paulo University – USP, Bauru School of Dentistry, Bauru, SP, Brazil. Al. Dr. Octavio Pinheiro Brizola, 9-75, Bauru, SP, Brazil. Postal code: 17012-901.

Ester Alves Ferreira Bordini

DDS, MS, PhD Department of Operative Dentistry, Endodontics and Dental Materials, Sao Paulo University – USP, Bauru School of Dentistry, Bauru, SP, Brazil. Al. Dr. Octavio Pinheiro Brizola, 9-75, Bauru, SP, Brazil. Postal code: 17012-901.

Marjorie de Oliveira Gallinari

DDS, MS, PhD, Department of Physiology and Pathology, Univ. Estadual Paulista – UNESP, Araraquara School of Dentistry, Araraquara, SP, Brazil. Humaita Street, 1680, Araraquara, SP, Brazil. Postal code: 14801-903.

Carlos Alberto de Souza Costa

DDS, MS, PhD, Professor, Department of Physiology and Pathology, Univ. Estadual Paulista – UNESP, Araraquara School of Dentistry, Araraquara, SP, Brazil. Humaitá Street, 1680, Araraquara, SP, Brazil. Postal code: 14801-903.

Diana Gabriela Soares

DDS, Ms, PhD, Assistant Professor, Department of Operative Dentistry, Endodontics and Dental Materials, Sao Paulo University – USP, Bauru School of Dentistry, Bauru, SP, Brazil. Al. Dr. Octavio Pinheiro Brizola, 9-75, Bauru, SP, Brazil. Postal code: 17012-901.

Corresponding author:
Prof. Dr. Diana Gabriela Soares
Department of Operative Dentistry, Endodontics and Dental Materials,
Bauru School of Dentistry, University of Sao Paulo (USP), Sao Paulo, Brazil
Alameda Octavio Pinheiro Brisolla, 9-75
17012-901 Bauru, SP, BRAZIL
E-mail: dianasoares@fob.usp.br

Supported by Fundação de Amparo à Pesquisa do Estado de São Paulo (FAPESP) – Grant/Award Number: 2019/06884-4; Coordenação de Aperfeiçoamento de Pessoal de Nível Superior - Brasil (CAPES) - Finance Code: 001

ABSTRACT

Mineral-induced bubbling effect and biomineralization as strategies to create highly porous and bioactive scaffolds for dentin tissue engineering

In this study, porous chitosan scaffolds were prepared by the mineral-induced bubbling-effect technique and subjected to biomineralization to create biomimetic scaffolds for dentin tissue engineering. Suspensions containing calcium hydroxide, nanohydroxyapatite, or β-tricalcium phosphate were added to the chitosan (CH) solution and subjected to gradual freezing and freeze-drying to obtain CH-Ca, CH-nHA, and CH-βTCP porous scaffolds, respectively, by the bubbling effect. Then, scaffolds were incubated in Simulated Body Fluid (SBF) for 5 days at 37°C, under constant stirring, to promote calcium-phosphate (Ca-P) biomineralization. Scanning electron microscopy revealed increased pore size and porosity degree on mineral-containing scaffolds, with CH-Ca and CH-nHA presenting as round, well-distributed, and with an interconnected pore network. Nevertheless, incubation in SBF disrupted the porous architecture, except for CH-$\mathrm{Ca_{SBF}}$, leading to the deposition of Ca-P coverage, confirmed by Fourier Transform Infrared Spectroscopy analyses. All mineral-containing and SBF-treated formulations presented controlled degradation profiles and released calcium throughout 28 days. When human dental pulp cells (HDPCs) were seeded onto scaffold structures, the porous and interconnected porous architecture of CH-Ca, CH-nHA, and CH-$\mathrm{Ca_{SBF}}$ allowed cells to infiltrate and spread throughout the scaffold structure, whereas in other formulations cells were dispersed or agglomerated. It was possible to determine a positive effect on cell proliferation and odontogenic differentiation for mineral-containing formulations, intensely improved by biomineralization. A significant increase in mineralized matrix deposition (by 8.4 to 18.9 times) was observed for CH-$\mathrm{Ca_{SBF}}$, CH-$\mathrm{nHA_{SBF}}$, and CH-$\mathrm{\beta TCP_{SBF}}$ in comparison with plain CH. The bioactive effect on odontoblastic marker expression (ALP activity and mineralized matrix) was also observed for HDPCs continuously cultivated with conditioned medium obtained from scaffolds. Therefore, biomineralization of chitosan scaffolds containing different mineral phases was responsible for increasing the capacity for mineralized matrix deposition by pulpal cells, with potential for use in dentin tissue engineering.

KEYWORDS

Scaffold, chitosan, mineral, biomineralization, dentin, vital pulp therapy

1 | INTRODUCTION

Direct pulp-capping is a vital pulp therapy (VPT) that involves the application of biomaterials over the exposed pulp in an attempt to achieve tissue regeneration mediated by the intrinsic regenerative potential of resident dental pulp stem cells. This therapy aims to recover and maintain normal function and vitality of this tissue through the odontoblastic differentiation and deposition of dentin by these cells, creating a mineralized barrier capable of sealing pulp from exposure (da Rosa et al., 2018; Zaen El-Din et al., 2020). Calcium hydroxide and calcium silicate cements/powder have been widely used for applications in VPT. However, their solubility, lack of adhesion, and low mechanical properties are considered concerns for long-term maintenance. Also, direct contact with these materials results in superficial necrosis and inflammation in remnant pulp tissue, resulting in a disorganized reparative process and establishment of a mineralized barrier with defects that may compromise dental pulp vitality. Therefore, tissue-engineering strategies have been proposed in the field of regenerative dentistry to overcome these clinical issues relative to current VPT techniques (da Rosa et al., 2018; Widbiller & Schmalz, 2021).

Dentin tissue-engineering proposes the development of materials with the ability to induce dentin repair/regeneration through the activation of the tertiary dentinogenesis process from resident pulpal and periapical stem cells, in a cell-homing pathway (Widbiller & Schmalz, 2021; Soares, Bordini, Swanson, de Souza Costa, & Bottino, 2021). Scaffolds play a crucial role in this process, since they serve as a framework for tissue neo-genesis. Moreover, they must modulate the chemotaxis events of resident cells to their structure, followed by their adhesion, spreading, infiltration, proliferation, cell differentiation, and the stimulation of secretory activity (Piva, Silva, & Nör, 2014; Galler, Eidt, & Schmalz, 2014; Soares et al., 2018a). In this sense, biomaterials with a composition similar to that of dentin have been proposed as an alternative to direct pulp-capping. Chitosan-based scaffolds demonstrate cytocompatibility and bioactivity with dental pulp cells, allowing for adequate cell interaction and inducing the processes of chemotaxis and mineralized matrix deposition in vitro and in vivo (Li, Liu, Zhao, Wu, & Xu, 2014; Soares et al., 2018a). The chemical composition of chitosan has shown an affinity for anionic biomolecules, such as the glycosaminoglycans of host extracellular matrix, and also allows for various possibilities for covalent and ionic modifications, including the incorporation of calcium and phosphate to create biomimetic scaffolds for mineralized tissue regeneration, thus adding the characteristic of versatility to this biopolymer (Madihally & Matthew, 1999; Ribeiro, Vieira, Melo, Araújo, & Lima, 2017; Islam, Shahruzzaman, Biswas, Nurus Sakib, & Rashid, 2020).

In addition to chemical composition, the three-dimensional (3D) architecture of scaffolds is critical to the regenerative process. Thus, scaffolds with a high degree of porosity and structure with interconnected pores are essential for favoring regeneration (Wei & Ma, 2006; Soares et al., 2018b; Soares, Bordini, Swanson, de Souza Costa, & Bottino, 2021). Chitosan solutions can be easily processed into porous scaffolds by phase-separation. Although widely used, this technique does not provide adequate control of pore size and interconnectivity (Madihally & Matthew, 1999; Pestov & Bratskaya, 2016). However, a bubbling-effect technique developed by our group facilitated the creation of an ordered and interconnected macro-pore network in chitosan scaffolds (Soares et al., 2020). Calcium hydroxide was incorporated into chitosan solution, acting as a CO_2 source upon carbonation and reaction with acetic acid, increasing pore diameter and total porosity during the gradual freezing procedure (Soares et al., 2020). The macro-porous structure obtained after freeze-drying allowed cells from surrounding in vitro 3D-matrices and in vivo tissues to easily infiltrate and spread inside and throughout the scaffold structure, denoting its potential as an inductive cell-homing platform (Soares et al., 2021). Furthermore, calcium was complexed to chitosan, creating the chitosan-calcium (CH-Ca) scaffold, which also acted as a calcium-release system capable of increasing the odontogenic potential of human dental pulp cells by increasing the deposition of mineralized tissue (Soares et al., 2020).

Based on the results obtained by our group, we hypothesized that other mineral phases could also promote the bubbling effect, generating a conductive surface that would favor tissue formation and growth. In this context, calcium phosphates have been extensively studied as biomaterials for their favorable characteristics such as biocompatibility, bioactivity, the absence of toxicity, variable degradation rates, and osteoconductivity (Guastaldi & Aparecida, 2010). For this reason, scaffolds containing hydroxyapatite (HA) [$Ca_{10}(PO_4)_6(OH)_2$] and β-tricalcium phosphate (βTCP) [$Ca_3(PO_4)_2$] have been investigated in tissue engineering, and their applications have also been suggested for targeting odontogenic differentiation (AbdulQader, Kannan, Rahman, Ismail, & Mahmood, 2015; Li et al., 2020; Cao et al., 2020; Guerrero-Gironés et al., 2021). This addition can improve the uniformity of osteoblastic cell-spreading and bone tissue formation when compared with that in non-combined materials, because the similarity to a bone/dentin extracellular matrix leads to enhanced interaction with precursor cells, as well as increasing the expression of some important bone markers, such as osteocalcin and bone sialoprotein, and improving the mechanical strength of scaffolds (Zhang & Ma, 2004; Kasten et al., 2008; Liu, Holzwarth, & Ma, 2012; Kim et al., 2015; AbdulQader, Kannan, Rahman, Ismail, & Mahmood, 2015; Goodarzi, Hashemi-Najafabadi, Baheiraei, & Bagheri, 2019; Wang, Lin, & Kang, 2019; Guerrero-Gironés et al., 2021).

Surface morphology should also be taken into consideration because it will exert a direct impact on cell adhesion, proliferation, and differentiation. An increase in the capacity for mineralized tissue deposition has already been demonstrated when mesenchymal stem cells adhere to surfaces with defined topography compared with smooth surfaces (Hu et al., 2010; Zhang, Hu, & Ma, 2012). The incubation of scaffolds in Simulated Body Fluid (SBF), a solution with composition, pH, temperature, and ionic concentration similar to those of human blood plasma, has been used as a biomineralization technique to modify the surfaces of scaffolds through the deposition of partially carbonated hydroxyapatite, mimicking the biological process of bone and tooth formation (Kokubo & Takadama, 2006). This biomimetic approach aims to modify the internal pore walls without changing the structure and properties of the scaffolds (Zhang & Ma, 2004; Wei & Ma, 2006). In this sense, this process can be used as a simple surface-modification technique for scaffolds used in bone and dentin tissue-engineering (Murphy, Kohn, & Mooney, 2000; Zhang & Ma, 2004).

Since the inorganic portion of dentin consists of mineral salts in the form of hydroxyapatite crystals, and calcium-based materials have been used for mineralized tissue regeneration, it can be suggested that the addition of mineral phases such as calcium hydroxide, HA, and βTCP to chitosan scaffolds, followed by biomineralization in SBF, could increase the bioactive potential of these biomaterials. Therefore, the objective of this work was to develop chitosan-based scaffolds enriched by mineral phases and biomineralized in SBF capable of activating the dentinogenic phenotype on human dental pulp cells, leading to dentin repair.

2 | MATERIALS AND METHODS

2.1 | Formulation and characterization of scaffolds

2.1.1 | *Synthesis of scaffolds*

All solutions described in this section are from the same manufacturer (Sigma-Aldrich Corporation, St. Louis, MO, USA), and the fabrication process followed the bubbling-effect technique established by our group (Soares et al., 2020). A solution of 2% (w/v) high-molecular-weight CH (310,000-375,000 Da; 75-80% deacetylated; pH 3.5) was prepared by the dissolution of chitosan powder in 2% (v/v) acetic acid solution under stirring for 24 hr. Then, 1% (w/v) aqueous suspensions of calcium hydroxide [$Ca(OH)_2$], nanohydroxyapatite (nHA; < 200 nm), and β-tricalcium phosphate (βTCP) were incorporated (separately) into chitosan solution by dripping at a 1:2 ratio and under 1000 rpm stirring for 5 min. The prepared solutions (CH, CH-Ca, CH-nHA, and CH-βTCP) were added to acrylic molds and subjected to a phase-separation process at low temperatures with gradual freezing in a -20°C freezer for 4 hr, overnight at -80°C, followed by immersion in liquid nitrogen at -198°C for 30 min. Afterward, the samples were freeze-dried at -84°C for 24 hr (FreeZone, Labconco Corporation, Kansas

City, MO, USA). Scaffolds 6 mm in diameter and 3 mm thick were obtained by means of a biopsy punch (Kolplast ci LTDA.; Itupeva, SP, Brazil). The samples were then subjected to the cross-linking process in 25% glutaraldehyde vapor for 6 hr. This protocol can modulate degradability while maintaining the porous architecture of the material after immersion in a liquid medium and does not cause cytotoxicity (Soares et al., 2020).

2.1.2 | *Biomineralization procedure in SBF*

The SBF solution was prepared as described by Kokubo and Takadama (2006), with an inorganic ion concentration 1.5 times that of human blood plasma, previously established by Wei and Ma (2006). Before incubation, the scaffolds were stabilized by immersion in 70% ethanol, followed by vacuum incubation for 30 min for the elimination of bubbles. Then, they were washed in phosphate-buffered saline (PBS; pH 7.4, Gibco®, Invitrogen™, Carlsbad, CA, USA). The scaffolds from each group were immersed in SBF solution and incubated for 5 days at 37°C under 100 rpm agitation, and the solution was renewed every 48 hr. The scaffolds were removed from the solution and immersed in deionized water for 24 hr for the removal of insoluble inorganic ions (Zhang & Ma, 2004), then gently dried with an absorbent paper towel and frozen at -20°C. They were then freeze-dried at -84°C overnight. The groups subjected to biomineralization were named CH_{SBF}, $CH\text{-}Ca_{SBF}$, $CH\text{-}nHA_{SBF}$, and $CH\text{-}\beta TCP_{SBF}$. The procedure for scaffold manufacturing is demonstrated in Figure 1a-1c.

2.1.3 | *Characterization of morphology and porosity*

The surface topography of the scaffolds subjected or not to incubation in SBF was evaluated under a Scanning Electron Microscope (SEM; PSEM eXpress, Aspex Corporation, Delmont, PA, USA). For this, the samples were positioned in stubs with carbon tape and coated with gold. The analyses were performed at an accelerating voltage of 15 kV with magnifications from 100x to 2500x. The porosity of the scaffolds (%) and pore diameter (µm; 115 units/sample) were calculated (n = 3) by means of ImageJ software (National Institutes of Health, Bethesda, MD, USA),

2.1.4 | *Chemical structure characterization*

The chemical structure was evaluated by Fourier Transform Infrared Spectroscopy (FTIR) in the Attenuated Total Reflectance (ATR) mode by means of Shimadzu FT-IR-8300 equipment

(Shimadzu Corporation, Kyoto, Honshu, Japan). Three samples from each group were placed in a standard position by means of a low-pressure press (Shimadzu Corporation) on the diamond crystal ATR (Smart Miracle^{TM}, Pike Technologies, Madison, WI, USA). Three readings were taken with an average of 32 scans between 4500 and 400 cm^{-1} and a resolution of 4 cm^{-1} at room temperature.

2.1.5 | *Degree of degradability of scaffolds*

The degree of degradability (DG) of the materials incubated or not in SBF was evaluated by calculation of the mass loss over 28 days (*n* = 6) by the wet-weight technique. The samples were incubated in 500 μL of PBS at 37°C for 1 hr. Subsequently, they were dried with absorbent paper for 15 min, and the initial wet weight (baseline) was measured on a precision electronic balance (MG214Ai 220g; Bel Engineering, Monza, MB, Italy). The samples were then incubated for 28 days at 37°C, with the PBS solution being renewed weekly. The weight was measured again after 1, 7, 14, 21, and 28 days of incubation. The DG was determined according to the formula DG (%) = ((Pf-Pi)/Pi)) x 100, where Pi represents the initial wet weight and Pf the final wet weight after immersion in PBS.

2.1.6 | *Calcium release*

This analysis was performed by immersion of the samples in 200 μL of ultrapure distilled water (Life Technologies, Carlsbad, CA, USA), pH 7.2, and at 37ºC for 1, 7, 14, and 21 days (*n* = 3). At each time-point, an aliquot was removed for reading by reaction with the o-cresolphthalein complexone substrate (Labtest Diagnóstica S.A., Lagoa Santa, MG, Brazil). Absorbance was quantified at 570 nm (Synergy Mx; BioTek Instruments, Winooski, VT, USA), and the data were converted into concentration (mg/dL) on a standard curve.

2.2 | Biological analysis in vitro

2.2.1 | *Culture of Human Dental Pulp Cells (HDPCs)*

HDPCs were obtained as previously described by Soares et al. (2018) after ethics approval (Human Research Ethics Committee - Bauru School of Dentistry, University of São Paulo - USP - CAAE 26153119.6.0000.5417). Briefly, the pulp tissue was collected from three sound third molars (one donor; 20 years old) and subjected to enzymatic disaggregation in collagenase type I solution (3 mg/mL, Sigma-Aldrich). Following an adhesion phase of 3 hr, the cells were subcultivated in fresh complete α-MEM (alpha Minimum Essential Medium, supplemented with 10% fetal bovine serum [FBS], L-glutamine, and 1% penicillin-streptomycin; GIBCO, Invitrogen, Carlsbad, CA, USA). Cells at passages 4-6 were used in this study.

2.2.2 | *Direct contact analysis*

The scaffolds were sterilized in 70% ethanol for 30 min, followed by the removal of internal bubbles in a vacuum. Then, samples were positioned in 48-well plates containing 500 µL of PBS. Residual ethanol was removed with three 15-minute baths in PBS, followed by overnight incubation in complete α-MEM culture medium (GIBCO®, Invitrogen) at 37°C and 5% CO_2. The medium was gently aspirated from the scaffolds, and cells (1 x 10^5 cells) were seeded in a 5-µL drop over the samples to avoid cell spillage onto the culture plate (Figure 1d). The cell/scaffold constructs were incubated at 37°C and 5% CO_2 for 30 min to allow for initial adhesion. Then, a 500-µL quantity of complete α-MEM culture medium was added, followed by 24-hour cultivation. Thereafter, the constructs were cultivated in complete α-MEM for cell viability analysis, or in an osteogenic medium (complete α-MEM supplemented with 50 mM ascorbic acid; 10 mM β-glycerophosphate; Sigma-Aldrich) for the alkaline phosphatase (ALP activity) and mineralized matrix deposition (Alizarin Red) assays. The analyses described below were performed with two independent experiments to ensure reproducibility of the results.

(a) Cell viability: After 1, 3, 7, and 14 days of culture, the scaffolds (*n* = 2) were washed in PBS and incubated with culture medium supplemented with Calcein AM and Ethyl Homodimer-1 (Live/Dead® Viability/Cytotoxicity Kit; Invitrogen, Carlsbad, CA, USA) at a concentration of 1:1000 for 15 min. Then, the presence of viable and dead cells on scaffolds was analyzed under a fluorescence microscope (FLoid, Life Technologies, Carlsbad, CA, USA).

(b) Quantification of cell viability (Alamar Blue): The Alamar Blue assay was performed after 1, 7, and 14 days of culture to quantify cell viability in the different periods, indirectly measuring cell proliferation. In each analysis, the constructs (*n* = 6) were incubated for 3 hr at 37°C and 5% CO_2 with the Alamar Blue® reagent (Life Technologies, Carlsbad, CA, USA) diluted in α-MEM without serum (1:10). After this period, the supernatant was transferred to 96-well plates and analyzed in a fluorescence reader (540 nm excitation - 590 nm emission; Synergy Mx; BioTek Instruments, Winooski, VT, USA). The data were normalized based on the control group (CH), and the viability of the control group was considered as 100% in each period.

(c) ALP activity: ALP activity was measured at 7 and 14 days of culture by means of the Alkaline Phosphatase kit (Labtest Diagnóstica S.A.; Lagoa Santa, MG, Brazil). The scaffolds (*n* = 6)

were washed with PBS, transferred to 1.5-mL tubes, and incubated in 0.1% sodium lauryl sulfate solution for 40 min. Then, the samples were cut and macerated, and 100 µL of buffer and 10 µL of substrate were added to each tube, followed by incubation for 15 min at 37°C. Subsequently, a 400-µL quantity of color reagent was added to each tube, which was then centrifuged at 12,000 rpm for 5 min. A 200-µL aliquot of the supernatant from each tube was transferred to a 96-well plate, and the absorbance was read at 590 nm (Synergy Mx; BioTek Instruments, Winooski, VT, USA). The data were obtained according to a standard curve and normalized by the total protein concentration method (Lowry/Folin-Ciocalteu method; Soares et al., 2020). The results were normalized by the volume (mm^3) of the scaffolds. The CH group was considered as 100% of ALP activity.

(d) Mineralized matrix deposition (Alizarin Red): After 14 and 21 days of culture, the scaffolds (*n* = 6) were washed with PBS and fixed in 70% ethanol at 4°C overnight. Then, they were washed in PBS and incubated for 20 min in Alizarin Red solution (40 mM, pH 4.2; Sigma-Aldrich). The scaffolds were washed with deionized water to remove excess dye and transferred to 1.5-mL tubes containing 500 µL of 10% cetylpyridinium chloride solution to dissolve the deposited minerals. The tubes were centrifuged at 4000 rpm for 2 min, and a 150-µL quantity of supernatant was collected from each tube and transferred to a 96-well plate for absorbance reading at 570 nm (Synergy Mx, BioTek, Winooski, VT, USA). Cell-free scaffolds were used to eliminate the background. The results were normalized by the volume (mm^3) of each sample of scaffolds. The CH group was considered as 100% of mineralized matrix deposition.

2.2.3 | *Biological analysis of scaffolds at a distance: cell-homing applicability (indirect method)*

For evaluation of the effects of the compounds released by the samples, scaffolds incubated or not in SBF were later incubated in osteogenic medium at 37°C and 5% CO_2 for up to 21 days to obtain a conditioned medium (extracts; *n* = 6), which was applied to the cells every 24 hr. On the day of incubation of the scaffolds, HDPCs (1.5 x 10^3 cells) were seeded in 96-well plates and cultured in complete α-MEM at 37°C and 5% CO_2 for 24 hr. Then, the cell medium was replaced with the 24-hour extracts and renewed with the new extracts obtained daily (Figure 1d). ALP activity was measured after 7 and 14 days, and mineralized matrix deposition (Alizarin Red) at 14 and 21 days, according to the protocol described previously, except for the maceration and centrifugation steps, since measurement was performed directly on the plate where the cells were seeded.

2.3 | Statistical analysis

Data from independent experiments were compiled and analyzed by one- or two-way ANOVA complemented by Tukey's or Dunnett´s test for observation of the significant differences between the study groups ($p < .05$ = statistically significant).

3 | RESULTS

3.1 | Physical/chemical characterization of the scaffolds

3.1.1 | *Scaffold architecture*

The SEM images of scaffolds incubated or not in SBF and subjected to the lyophilization procedure are presented in Figure 2. CH presented a disorganized porous architecture, whereas the addition of mineral phases to CH was responsible for creating larger pores. This effect was more evident for CH-Ca and CH-nHA, in which an organized macro-pore network was observed, with round pores. CH-βTCP presented a less organized architecture but with larger pores than CH. Incubation in SBF altered CH scaffold architecture, in which it was possible to observe the presence of a discrete and almost imperceptible coating on the external surface. CH-Ca_{SBF} retained the macro-porous architecture, and disperse mineral-like deposits could be observed on its structure. Nevertheless, CH-nHA_{SBF} and CH-βTCP_{SBF} presented a disorganized architecture and the presence of large mineral deposits on their surfaces, which was more evident for CH-nHA_{SBF}.

3.1.2 | *Chemical composition*

Figure 3a shows the FTIR spectra of the reference spectra of $Ca(OH)_2$, nHA, and βTCP, and for the materials after the incorporation of $Ca(OH)_2$, nHA, and βTCP into chitosan. The $Ca(OH)_2$ spectrum showed characteristic bands at 3640 cm^{-1} and a strong band at 500 cm^{-1}, corresponding to O─H and Ca-O stretching vibrations, respectively. The reference spectra of the nHA and βTCP mineral phases showed characteristic strong bands, easily distinguished and assigned to the PO_4^{-3} groups, referring to stretching and angular vibrations. The bands at 1102 cm^{-1} and 1040 cm^{-1} were assigned to asymmetric -P-O stretching components, triply degenerate. The band at 964 cm^{-1} was assigned to symmetric -P-O stretching modes. The components of the angular -O-P-O- triply degenerate vibration mode were assigned bands at 601 cm^{-1} and 570 cm^{-1} for HA and 601-588 cm^{-1} and 540 cm^{-1} for βTCP. The angular -O-P-O- double-degenerate modes of vibration were in the range 462-474 cm^{-1}. The weak band could appear at 875 cm^{-1}, referring to HPO_4^{-2}. The band at 3400 cm^{-1} refers to the symmetric -OH stretching of the structure (Ślósarczyk, Paluszkiewicz, Gawlicki, & Paszkiewicz, 1997). The bands at 3560 cm^{-1} and 632 cm^{1}, corresponding to the -OH structure, were present in apatite (HA) and absent in β-TCP precursors.

It was possible to observe the characteristic absorption bands for the CH scaffold (Jeon, & Höll, 2003; Amaral, Granja, & Barbosa, 2005; Yuan, Shah, Hein, & Misra, 2010; Zeng et al., 2011; Thomas et al., 2018). The changes in the wavelengths and intensities of the characteristic bands indicated the chemical changes in the structures of the CH-Ca, CH-nHA, and CH-βTCP scaffolds as a function of the addition of the mineral phases. It was possible to notice, through the extended region, changes in the 1640, 1606, 1550, 1443, 1413, 1381, 1315, and 1066 cm^{-1} bands relative to the -N-H stretching, amine, and amide vibrations (-NH2, -NHCO, -C-N) and C-O stretching, indicating the involvement of the amino and C-O groups in the complexation with ions from the added mineral phases, such as calcium or phosphate groupings, as a function of the changes in the absorption bands at 1066, 1028, and 655 cm^{-1}.

Figure 3b-3e presents the comparison of FTIR spectra of the scaffolds of the CH, CH-Ca, CH-nHA, and CH-βTCP groups, before and after immersion in SBF solution, for evaluation of the biomineralization characteristics indicative of hydroxyapatite deposition. As mentioned previously, the reference spectrum of HA shows that characteristic bands for PO_4^{-3} groups could be observed at 472, 566, 601, 960, 1027, and 1100 cm^{-1}. The bands corresponding to the structural -OH groups of apatite were assigned at 630 cm^{-1} and 3560 cm^{-1} (Cardenas-Triviño & Carrasco-Garcia, 2019). It was possible to notice differences in the main amide I, II, and III bands, with significant variations in intensities and positions. There was a significant change in the 1120-975 cm^{-1} regions, referring to the stretching of -C-O groups of the chitosan structure. Another significant change occurred in the 620-558 cm^{-1} region, where prominent new absorption bands were noted located at 1022, 601, and 559 cm^{-1}, consistent with the prominent absorption bands of hydroxyapatite, referring to the phosphate groups present in the structure (Danylchenko, Kalinkevich, & Pogorelov, 2009).

3.1.3 | *Pore size and porosity degree*

Analysis of SEM images indicated that CH-Ca and CH-βTCP featured the largest pore diameters, whereas the other groups presented similar pore sizes in comparison with CH (Figure 4a). Nevertheless, calculation of the degrees of porosity (Figure 4b) indicated that all mineral phases increased the percentage of porosity statistically significantly in comparison with CH, with CH-Ca and CH-Ca_{SBF} showing the highest values, followed by CH-βTCP and

CH-nHA. In contrast, SBF treatment intensely reduced the degrees of porosity of CH-nHA$_{SBF}$ and CH-βTCP$_{SBF}$.

3.1.4 | *Calcium release and degradation profile*

The cumulative calcium (Ca^{2+}) release profile of the scaffolds is shown in Figure 4c. The CH-nHA and CH-βTCP scaffolds subjected or not to SBF treatment had the highest release at all time-points, with a cumulative profile throughout 21 days. CH-Ca had a peak of Ca^{2+} release at 7 days that was not detected on CH-Ca$_{SBF}$. Regarding the degradation profile (Figure 4d), CH showed no alteration in wet mass throughout the 28-day period. The addition of mineral phases led to a high degradation rate of the scaffolds when immersed in a neutral aqueous medium starting at 7 days for CH-βTCP and CH-βTCP$_{SBF}$, and at 14 days for CH-Ca, CH-nHA, and CH-nHA$_{SBF}$. Incubation of CH and CH-Ca in SBF resulted in no difference in wet weight over time when compared with their respective baselines.

3.2 | In vitro biological characterization

3.2.1 | *Direct contact assay*

For all experimental groups, the cells remained viable and were able to proliferate over time, as demonstrated by Live/Dead and Alamar Blue assays (Figure 5), indicating that all formulations were cytocompatible. It was possible to observe, in Live/Dead images (Figure 5a), that CH-Ca and CH-nHA cells spread throughout the scaffold structure at 14 days, presenting a stretched cytoplasm, where cells in the CH group were dispersed on the material structure. Cells in CH-βTCP had a tendency to form agglomerates. The stretched cell architecture could also be noted on CH-Ca$_{SBF}$ at the 14-day period; nevertheless, cell agglomerates were observed for the CH-nHA$_{SBF}$ and CH-βTCP$_{SBF}$ groups. It was also possible to observe a higher cell density on CH-Ca, CHnHA, and CH-βTCP formulations, subjected or not to SBF treatment, in comparison with that of CH and CH$_{SBF}$ groups, starting at 7 days. The Alamar Blue assay (Figure 5b) detected increased cell viability values for mineral-rich SBF-treated groups at 7 days, and for all experimental groups at 14 days, in comparison with those of the CH group. A considerable increase in viability was observed at 7 and 14 days compared with the CH group for the formulations incubated in SBF, especially in the CH-nHA$_{SBF}$ and CH-βTCP$_{SBF}$ groups. There was an increase in ALP activity for all groups over time (Figure 5c). The addition of mineral phases did not affect the ALP activity of the groups compared with the CH control. Incubation in SBF increased ALP activity for all mineral-rich SBF-treated groups in both periods of analysis. The positive effect of mineral phase incorporation in association with SBF treatment was also detected in the Alizarin Red assay (Figure 5d). Incorporation of a mineral phase alone promoted significant increases in mineralized matrix deposition at 14 days in comparison with the CH group by 1.9 to 2.4 times; nevertheless, association with SBF treatment led to increases of 9.8, 18.9, and 8.4 times in mineralized matrix deposition for the CH-Ca_{SBF}, CH-nHA_{SBF}, and CH-βTCP_{SBF} groups, respectively, in comparison with CH.

3.2.2 | *Effects of conditioned medium*

In evaluation of the effects of the compounds released by the samples over HDPC activity, it was possible to observe higher ALP activity at 14 days for all groups after the addition of the mineral phases when compared with the CH control (Figure 6a). Incubation in SBF increased the ALP activity in all groups at 14 days compared with the CH control, and also with respective formulations with no SBF treatment. Regarding mineralized matrix deposition (Figure 6b), the addition of mineral phases led to increased deposition in the CH-Ca and CH-β-TCP groups at 21 days compared with the CH control group. Incubation in SBF increased deposition at 21 days for all groups compared with the CH control group.

4 | DISCUSSION

Currently, there are increasing efforts to modulate tissue regeneration by the development of biomaterials that can adapt to the biological microenvironment where they are inserted, inducing specific cellular responses that optimize the repair process (Ahmed, Abouauf, AbuBakr, Dörfer, & El-Sayed, 2020; Bottino, Pankajakshan, & Nör, 2017). In the present study, we proposed the fabrication of chitosan scaffolds associated with different mineral phases and subjected to a biomineralization process in SBF, to create biomimetic scaffolds for application in direct pulp-capping. Phase-separation is a simple method to form chitosan scaffolds by segregating the polymeric phase during freezing, followed by ice elimination via freeze-drying. However, this technique provides no control over the degree of porosity (Madihally & Matthew, 1999; Zhu, Wan, Zhang, Yin, & Cheng, 2014; Aranaz et al., 2017). Therefore, in this study we applied a manufacturing method previously developed by our group (Soares et al., 2020), in which a $Ca(OH)_2$ suspension is added to the CH solution under stirring, at a 1:2 ratio, creating highly porous scaffolds with increased and organized pores in comparison with pure chitosan scaffolds. The other mineral phases used in this study, βTCP and nHA, were incorporated in the same way and at the same proportions, and the effects of these incorporations were analyzed.

According to our results, $Ca(OH)_2$, nHA, and βTCP were capable of modulating the porous architecture of chitosan scaffolds, increasing pore size and overall porosity. Nevertheless, only CH-Ca and CH-nHA had a round and well-distributed porous network, with an interconnected porous structure. Incorporation of βTCP created an open pore structure, albeit with a disorganized architecture. CH-Ca had the highest pore size and porosity degree, followed by CH-βTCP and CH-nHA. The mechanisms related to porous architecture mediated by $Ca(OH)_2$ were a consequence of CO_2 release during the slow and gradual freezing process, resulting in bubbles that underwent expansion within the polymeric mesh (bubbling effect), creating the round and interconnected pores. The incorporation of $Ca(OH)_2$ acted as the CO_2 source upon carbonation and reactions with acetic acid, increasing the pore diameter and total porosity compared with those of plain chitosan scaffolds (Soares et al., 2020). Therefore, based on our results, we believe that βTCP and nHA also promoted a bubbling effect upon incorporation into chitosan solution, leading to pore enlargement as observed by SEM images. Kim et al. (2015) obtained similar results by incorporating alginate-nHA dispersion into a 4% chitosan solution in a 1% acetic aqueous solution, avoiding the occurrence of mineral agglomerates. A clear chitosan/alginate/nHA solution was obtained, which was then gradually frozen from 4°C to -20°C, and freeze-dried at -89°C. A chitosan scaffold showing a homogeneous round pore network, with pore size varying from 100 to 400 μm, and porosity higher than 80%, was achieved, whereas the plain chitosan solution resulted in a lamellar pore network. Other researchers also demonstrated that an acid-base reaction of citric acid with $NaHCO_3$ produced CO_2 bubbles in $CaCO_3$ scaffolds, giving rise to an organized macro-porous architecture (Chen et al., 2012; Thein-Han, & Xu, 2013; Chen, Thein-Han, Weir, Chen, & Xu, 2014).

Besides modulating overall scaffold architecture, the $Ca(OH)_2$ mineral-induced bubbling effect also led to calcium (Ca^{2+}) complexation to chitosan, creating the CH-Ca scaffold, which also acted as a calcium-release system capable of increasing the odontogenic potential of human dental pulp cells by increasing the deposition of mineralized tissue (Soares et al., 2020). The FTIR analysis of current formulations confirmed that Ca^{2+} was indeed complexed to chitosan on CH-Ca, and also demonstrated that Ca^{2+} and PO_4^{3-} were incorporated into chitosan on CH-βTCP and CH-nHA. Upon incubation of an apatite source in acid solution, the dissolution process occurred, in which H+ and anions of acid from the bulk solution promoted the release of Ca^{2+} and PO_4^{3-} from mineral surfaces (Dorozhkin, 2012). These ions were susceptible to chemical interaction in the amino, hydroxyl, and acetyl groups of the chitosan molecule (Pestov & Bratskaya, 2016; Shakir et al., 2015; Kar, Kaur, & Thirugnanam, 2016; Keikhaei, Mohammadalizadeh, Karbasi, & Salimi, 2019). Our results also suggested these interactions. The changes regarding -N-H stretching, amine and amide vibrations, and C-O stretching demonstrate the involvement of these groups in the complexation of the Ca^{2+} and PO_4^{3-} ions present in the added suspensions.

In addition to the incorporation of $Ca(OH)_2$, βTCP, and nHA as bioactive mineral phases, in this study we used a biomimetic mineralization technique for manufacturing the biomaterials. This technique is based on the incubation of the samples in SBF, a solution with ions in concentrations similar to those found in human blood plasma. Rich in Ca^{2+} and PO_4^{3}, this fluid can promote the formation of calcium phosphate (Ca-P) crystalline structures similar to the apatite found in native bone and has been used to improve the bone-regeneration properties of scaffolds by mimicking the natural bone surface, promoting an ideal environment for osteogenesis, and increasing the structural stability of the scaffold (Xin, Leng, Chen, & Zhang, 2005; Castro, Tan, Shen, & Zhang, 2016; Shin, Acri, Geary, & Salem, 2017).

SBF-mediated mineralization occurs in a series of events, beginning with the high concentrations of Ca^{2+} and PO_4^{3-} contained in the solution that form pre-nucleation crystals. The amorphous solids are then attracted to the polar surface groups of the substrate. The apatite crystals are deposited, and the formed apatite becomes a nucleation site, allowing more crystals to grow continuously (Shin, Acri, Geary, & Salem, 2017). Incubation parameters in SBF have undergone significant changes since its first formulation, to accelerate the deposition and coating of biomaterials. Thus, studies have evaluated factors such as concentration and composition of the solution, aiming to improve the surface-coating characteristics (Yuan, Mak, & Li, 2001; Wei & Ma, 2006; Guastaldi & Aparecida, 2010). A higher ionic concentration of the SBF solution facilitates apatite formation. In a study by Zhang and Ma (2004), incubation of polymeric scaffolds in SBF at a 1.5-fold concentration was responsible for higher apatite deposition compared with the conventional concentration, indicating that increasing the ionic concentration may be a practical way to facilitate apatite nucleation and growth, probably due to the higher availability of Ca^{2+} and PO_4^{3-} to be precipitated. Therefore, we selected this SBF concentration to promote Ca-P covering on our macro-porous scaffolds, which was confirmed by FTIR as indicative of hydroxyapatite, by the intense absorption bands corresponding to the phosphate groups observed in SBF-treated samples.

The scaffolds from the CH-nHA group subjected to biomineralization showed intense mineral coverage when compared with the other groups. This also occurred in a previous study, in which Wei and Ma (2006) demonstrated that pre-incorporation of nHA (even in low proportions) into poly(L-lactic acid) (PLLA)-based polymeric scaffolds induced greater apatite formation when in SBF compared with a pure polymeric scaffold. This can be explained by the higher ionic availability provided by the presence of nHA in the scaffold, which may have facilitated the formation of nucleation sites and allowed for greater crystal growth. This effect was also detected for CH-βTCP, since large mineral structures were detected on scaffold surfaces, whereas CH and CH-Ca showed only a slight, almost imperceptible mineral deposition. Therefore, Ca-P seems to play an important role as pre-nucleation for biomineralization to occur. Nevertheless, the porous structure of CH-nHA and CH-βTCP was intensely disrupted, which affected cell infiltration and spread throughout the scaffold structure. Only the CH-Ca scaffold subjected to SBF treatment maintained the macro-porous and interconnected network, as observed by SEM images, denoting the more stable and predictable architecture provided by the bubbling effect mediated by $Ca(OH)_2$.

An important parameter in tissue engineering is scaffold biodegradability, because, as a temporary structure, the scaffold must be replaced by new tissue (Murphy, Kohn, & Mooney, 2000). Therefore, the biomaterial must have a controlled rate of biodegradability, which must be consistent with the rate of new tissue formation (Ribeiro, Vieira, Melo, Araújo, & Lima, 2017; Islam, Shahruzzaman, Biswas, Nurus Sakib, & Rashid, 2020). In this study, the addition of mineral phases led to a higher scaffold degradation rate when immersed in a neutral aqueous medium. Overall, biomineralization was responsible for a slight increase in the percentage of this degradation, except for the $CH\text{-}Ca_{SBF}$ group. However, even with the loss of mass, the scaffolds of all groups remained viable for cell interaction throughout the 21 days of analysis in vitro, which was enough time to allow for cell differentiation and deposition of the mineralized matrix by the HDPCs, as proven by the results of the biological analyses that will be discussed further. In our previous in vivo study using CH-Ca in rat calvaria, the scaffold remained stable for mineralized tissue regeneration after the 30-day period, as detected by histological sections (Soares et al., 2021).

From a biological perspective, the incorporation of mineral phases into the chitosan scaffold is proposed to increase bioactivity and accelerate the formation of the mineralized matrix. In our first proposal, $Ca(OH)_2$ was selected, since it is the most common cement used for direct pulp-capping. Therefore, we were able to demonstrate that it was possible to create a bioactive matrix with a porous structure using this inexpensive mineral phase, capable of acting as a controlled calcium-release system. Using this tissue-engineering strategy, we were able to propose a 3D matrix capable of modulating tissue regeneration by stimulating resident pulp cells and boosting odontoblastic differentiation and mineralized matrix deposition (Soares et al., 2020). More recently, we also demonstrated that CH-Ca had a chemotactic potential with dental pulp cells, using an artificial pulp chamber model in vitro, in which we were able to demonstrate that cells migrated from a 3D culture in intimate contact with cell-free CH-Ca, infiltrating its porous network and expressing odontogenic-related proteins. This porous material also improved new bone deposition toward the centers of critical-sized defects in rat calvaria in vivo, demonstrating its potential as an inductive cell-homing platform for mineralized tissue regeneration, such as bone and dentin (Soares et al., 2021). These homing effects were related to Ca^{2+} released by biomaterials, resulting in an influx of Ca^{2+} in the intracellular environment through the activation of Ca^{2+} channels, which would increase the expression of genes related to odontogenic differentiation (An, Gao, Ling, Wei, & Xiao, 2012; Gandolfi et al., 2015; Kuzmenka et al., 2020). An et al. (2012) investigated the effects of different Ca^{2+} concentrations on the growth and odontogenic differentiation of HDPCs, concluding that the odontogenic properties of these cells can be influenced by the Ca^{2+} content present in the culture medium, and that, therefore, it is important to optimize the release of these ions for a better clinical outcome in pulp-capping materials. Chitosan-based vehicles targeting sustained Ca^{2+} release have been developed and have demonstrated an adequate calcium-release profile in addition to cytocompatibility (Farhadian, Godiny, Moradi, Azandaryani, & Shahlaei, 2018; Flores-Arriaga et al., 2019).

In the current study, we went a step further to demonstrate if traditional Ca-P sources, commonly used for bone regeneration, would result in better effects as bioactive tools in our manufacturing method. Due to the excellent results of βTCP and HA in bone regeneration, these mineral phases have also been proposed for dentin regeneration, with exciting results. AbdulQader et al. (2015) investigated the proliferation and differentiation of HDPCs under the effects of extracts obtained from scaffolds with different proportions of HA and β-TCP. Cells cultured with the extracts from scaffolds in the β-TCP at a 20/80 HA ratio showed high ALP activity and positive regulation of the expression levels of bone sialoprotein (BSP), dentin matrix protein-1 (DMP-1), and dentin sialophosphoprotein (DSPP), genes associated with the differentiation and maturation process of odontoblasts. In another in vitro study, immortalized HDPCs exhibited odontogenic differentiation and DSPP expression when combined with a scaffold of βTCP and bone morphogenetic protein (BMP2) (Li et al., 2020). Recently, Guerrero-Gironés et al. (2021) evaluated the effect of a scaffold containing βTCP, HA, and collagen (C) on the vital pulp of rat molars, comparing it with mineral trioxide aggregate (MTA), and demonstrated superior results on mineralized barrier deposition. Cao et al. (2020) analyzed two types of 3D-printed scaffolds, one based on poly(lactic acid-co-glycolic acid) in association with βTCP (3D-PLGA/β-TCP) and another based on βTCP (3D-TCP). Both formulations increased the adhesion and proliferation of HDPCs, and promoted odontogenic differentiation.

Therefore, we performed two in vitro assays to observe the biological activities of current formulations, by cultivating HDPCs directly on the scaffolds (direct contact) and exposing them to their extracts (remote). It was possible to observe that all formulations were cytocompatible and allowed cells to proliferate through time within the scaffold structure. An interesting find referred to cell spread throughout scaffold structure at the 14-day period, observed by the Live/Dead assay. This effect was more evident for CH-Ca and CH-nHA, which featured a round and interconnected macro-porous network. The macro-porous architecture of CH-βTCP resulted in cell agglomerates, but it was also possible to observe an interconnection among the clusters, which was not detected in the CH group. Following SBF treatment, we detected a disruption of the porous architecture of CH-nHA$_{SBF}$ and CH-βTCP$_{SBF}$ due to intense Ca-P deposition, which resulted in large cell agglomerates. Only CH-Ca$_{SBF}$ retained the macro-porous architecture, allowing for a better cell spread. Since the CH scaffold had a lower degree of porosity and disconnected porous architecture, the cells appeared dispersed on its surface. A positive effect of SBF treatment on cell proliferation was detected, since the Alamar Blue assay revealed a considerable increase in cell metabolism at 7 and 14 days for the groups containing mineral phases and incubated in SBF compared with the group with pure CH (control). According to the literature, this could be explained due to the formation of the Ca-P layer on the surface, promoting greater cell adhesion between the material and the cells by increasing surface roughness, surface area, and focal adhesion points (Boone et al., 1989; Castro, Tan, Shen, & Zhang, 2016).

Regarding odontogenic differentiation, it was possible to detect that $Ca(OH)_2$, nHA, and βTCP featured similar positive effects on ALP activity and mineralized matrix deposition by the cells seeded onto scaffold structures and cultivated with conditioned medium. This bioactive effect was significantly improved by SBF treatment. An intense increase in mineralized matrix deposition could be observed for the cells in direct contact with these biomineralized scaffolds. This effect was more prominent at the 21-day time-point, with CH-nHA$_{SBF}$ featuring the highest values, increasing by 18.9 times the mineralized matrix deposited by the cells. CH-Ca$_{SBF}$ and CH-βTCP$_{SBF}$ also had stunning results, up-regulating mineralized matrix deposition by 9.8 and 8.4 times, respectively. The mineral-containing scaffolds not treated with SBF led to increased mineralized matrix deposition by 1.9 to 2.4 times. For cells cultured with the components continuously released by the scaffolds, this mineral-induced effect was similar among mineral-containing scaffold formulations (up to 1.6 times), regardless of SBF treatment.

Other studies have shown similar results, indicating that incubation in SBF has the potential to increase cell viability. A collagen scaffold, subjected to HA coating through SBF immersion, demonstrated excellent biological performance in vitro, with potential for use in bone tissue engineering (Al-Munajjed et al., 2009). Castro et al. (2016) developed porous scaffolds 3D-printed from filaments of a polyurethane-based elastomeric composite. The material was incubated in SBF for different periods, resulting in adequate nucleation of hydroxyapatite, which was responsible for increasing nanoscale surface roughness without changing the structure of the material. The nucleation of hydroxyapatite facilitated cell adhesion and spreading within the first 24 hr; differentiation was also increased, and there was an increase in the deposition of the mineralized matrix when compared with that in the control group, without biomineralization.

Therefore, the addition of mineral phases and the biomineralization coating method proposed in this investigation appear to be promising approaches capable of increasing the bioactivity of chitosan-based scaffolds for use in dentin regeneration. Nevertheless, it is important to note that only $Ca(OH)_2$ and nHA were capable of promoting an adequate mineral-induced bubbling effect on chitosan scaffolds, resulting in a large, round, well-distributed, and interconnected porous network throughout the scaffold structure. These compositions had a bioactive effect, positively modulating the odontoblastic differentiation of HDPCs. Nevertheless, the biomineralization technique resulted in intense mineral deposits on nHA surfaces, disrupting the porous architecture and interfering with cell spread. Collective results suggest that the biomineralized CH-Ca formulation appears to be an interesting biomaterial for boosting dental pulp cell mineralization phenotypes, while maintaining the macro-porous architecture that is crucial for a cell-homing strategy. The significant advantage of this formulation is its lower cost relative to that of the other tested Ca-P mineral phase, and its simple fabrication process. Therefore, further studies are necessary to prove its potential as a designed scaffold applicable for dentin tissue engineering.

5 | CONCLUSIONS

This study demonstrated that the incorporation of proposed mineral phases as suspensions into chitosan solutions following a specific phase-separation route promotes a mineral-induced bubbling effect, modulating porous scaffold architecture, chemical composition, and degree of degradability, creating interesting porous and bioactive scaffolds for mineralized tissue regeneration. Also, biomineralization with SBF improved the bioactive potential of these formulations, regardless of the disruption of porous architecture in selected formulations. Overall, the CH-Ca scaffold subjected to biomineralization was the sole composition capable of maintaining the macro-porous architecture, being capable of boosting the proliferation and mineralizing phenotypes of dental pulp cells seeded onto its structure, and at a distance, similarly to traditional Ca-P phases, presenting the potential for the development of low-cost cell-free strategies for dentin tissue engineering.

ACKNOWLEDGMENTS

This work was supported by the Fundação de Amparo à Pesquisa do Estado de São Paulo (FAPESP) – Grant/Award Numbers 2016/15674-5 and 2019/06884-4, and by the Coordenação de Aperfeiçoamento de Pessoal de Nível Superior - Brasil (CAPES) - Finance Code 001.

REFERENCES

1. da Rosa, W., Cocco, A. R., Silva, T., Mesquita, L. C., Galarça, A. D., Silva, A., & Piva, E. (2018). Current trends and future perspectives of dental pulp capping materials: A systematic review. *Journal of biomedical materials research. Part B, Applied biomaterials*, *106*(3), 1358–1368. https://doi.org/10.1002/jbm.b.33934

2. Zaen El-Din, A. M., Hamama, H. H., Abo El-Elaa, M. A., Grawish, M. E., Mahmoud, S. H., & Neelakantan, P. (2020). The effect of four materials on direct pulp capping: An animal study. *Australian endodontic journal: the journal of the Australian Society of Endodontology Inc*, *46*(2), 249–256. https://doi.org/10.1111/aej.12400

3. Widbiller, M., & Schmalz, G. (2021). Endodontic regeneration: hard shell, soft core. *Odontology*, *109*(2), 303–312. https://doi.org/10.1007/s10266-020-00573-1

4. Soares, D. G., Bordini, E., Swanson, W. B., de Souza Costa, C. A., & Bottino, M. C. (2021). Platform technologies for regenerative endodontics from multifunctional biomaterials to tooth-on-a-chip strategies. *Clinical oral investigations*, *25*(8), 4749–4779. https://doi.org/10.1007/s00784-021-04013-4

5. Piva, E., Silva, A. F., & Nör, J. E. (2014). Functionalized scaffolds to control dental pulp stem cell fate. *Journal of endodontics*, *40*(4 Suppl), S33–S40. https://doi.org/10.1016/j.joen.2014.01.013

6. Galler, K. M., Eidt, A., & Schmalz, G. (2014). Cell-free approaches for dental pulp tissue engineering. *Journal of endodontics*, *40*(4 Suppl), S41–S45. https://doi.org/10.1016/j.joen.2014.01.014

7. Soares, D. G., Zhang, Z., Mohamed, F., Eyster, T. W., de Souza Costa, C. A., & Ma, P. X. (2018). Simvastatin and nanofibrous poly(l-lactic acid) scaffolds to promote the odontogenic potential of dental pulp cells in an inflammatory environment. *Acta biomaterialia*, *68*, 190–203. https://doi.org/10.1016/j.actbio.2017.12.037 (a)

8. Li, F., Liu, X., Zhao, S., Wu, H., & Xu, H. H. (2014). Porous chitosan bilayer membrane containing TGF-β1 loaded microspheres for pulp capping and reparative dentin formation in a dog model. *Dental materials : official publication of the Academy of Dental*

Materials, *30*(2), 172–181. https://doi.org/10.1016/j.dental.2013.11.005

9. Madihally, S. V., & Matthew, H. W. (1999). Porous chitosan scaffolds for tissue engineering. *Biomaterials*, *20*(12), 1133–1142. https://doi.org/10.1016/s0142-9612(99)00011-3

10. Ribeiro, J. C. V., Vieira, R. S., Melo, I. M., Araújo, V. M. A., & Lima, V. (2017). Versatility of Chitosan-Based Biomaterials and Their Use as Scaffolds for Tissue Regeneration. *The Scientific World Journal*, 2017, 25. https://doi.org/10.1155/2017/8639898

11. Islam, M. M., Shahruzzaman, M., Biswas, S., Nurus Sakib, M., & Rashid, T. U. (2020). Chitosan based bioactive materials in tissue engineering applications-A review. *Bioactive materials*, *5*(1), 164–183. https://doi.org/10.1016/j.bioactmat.2020.01.012

12. Wei, G., & Ma, P. X. (2006). Macroporous and nanofibrous polymer scaffolds and polymer/bone-like apatite composite scaffolds generated by sugar spheres. *Journal of biomedical materials research. Part A*, *78*(2), 306–315. https://doi.org/10.1002/jbm.a.30704

13. Soares, D. G., Anovazzi, G., Bordini, E., Zuta, U. O., Silva Leite, M., Basso, F. G., Hebling, J., & de Souza Costa, C. A. (2018). Biological Analysis of Simvastatin-releasing Chitosan Scaffold as a Cell-free System for Pulp-dentin Regeneration. *Journal of endodontics*, *44*(6), 971–976.e1. https://doi.org/10.1016/j.joen.2018.02.014 (b)

14. Pestov, A., & Bratskaya, S. (2016). Chitosan and Its Derivatives as Highly Efficient Polymer Ligands. *Molecules (Basel, Switzerland)*, *21*(3), 330. https://doi.org/10.3390/molecules21030330

15. Soares, D. G., Bordini, E., Cassiano, F. B., Bronze-Uhle, E. S., Pacheco, L. E., Zabeo, G., Hebling, J., Lisboa-Filho, P. N., Bottino, M. C., & de Souza Costa, C. A. (2020). Characterization of novel calcium hydroxide-mediated highly porous chitosan-calcium scaffolds for potential application in dentin tissue engineering. *Journal of biomedical materials research. Part B, Applied biomaterials*, *108*(6), 2546–2559. https://doi.org/10.1002/jbm.b.34586

16. Soares, D. G., Bordini, E., Bronze-Uhle, E. S., Cassiano, F. B., Silva, I., Gallinari, M. O., Matheus, H. R., Almeida, J. M., Cintra, L., Hebling, J., & de Souza Costa, C. A. (2021). Chitosan-Calcium-Simvastatin Scaffold as an Inductive Cell-Free Platform. *Journal of dental research*, *100*(10), 1118–1126. https://doi.org/10.1177/00220345211024207

17. Guastaldl, A. C., Aparecida, A. H. (2010). Fosfatos de cálcio de interesse biológico: importância como biomateriais, propriedades e métodos de obtenção de recobrimentos. *Quim. Nova*, 33 (6), 1352-1358. https://doi.org/10.1590/S0100-40422010000600025

18. AbdulQader, S. T., Kannan, T. P., Rahman, I. A., Ismail, H., & Mahmood, Z. (2015). Effect of different calcium phosphate scaffold ratios on odontogenic differentiation of human dental pulp cells. *Materials science & engineering. C, Materials for biological applications*, *49*, 225–233. https://doi.org/10.1016/j.msec.2014.12.070

19. Li, X., Wang, L., Su, Q., Ye, L., Zhou, X., Song, D., & Huang, D. (2020). Highly Proliferative Immortalized Human Dental Pulp Cells Retain the Odontogenic Phenotype when Combined with a Beta-Tricalcium Phosphate Scaffold and BMP2. *Stem cells international*, *2020*, 4534128. https://doi.org/10.1155/2020/4534128

20. Cao, S., Han, J., Sharma, N., Msallem, B., Jeong, W., Son, J., Kunz, C., Kang, H. W., & Thieringer, F. M. (2020). In Vitro Mechanical and Biological Properties of 3D Printed Polymer Composite and β-Tricalcium Phosphate Scaffold on Human Dental Pulp Stem Cells. *Materials (Basel, Switzerland)*, *13*(14), 3057. https://doi.org/10.3390/ma13143057

21. Guerrero-Gironés, J., Alcaina-Lorente, A., Ortiz-Ruiz, C., Ortiz-Ruiz, E., Pecci-Lloret, M. P., Ortiz-Ruiz, A. J., Rodríguez-Lozano, F. J., & Pecci-Lloret, M. R. (2021). Biocompatibility of a HA/β-TCP/C Scaffold as a Pulp-Capping Agent for Vital Pulp Treatment: An In Vivo Study in Rat Molars. *International journal of environmental research and public health*, *18*(8), 3936. https://doi.org/10.3390/ijerph18083936

22. Zhang, R., & Ma, P. X. (2004). Biomimetic polymer/apatite composite scaffolds for mineralized tissue engineering. *Macromolecular bioscience*, *4*(2), 100–111. https://doi.org/10.1002/mabi.200300017

23. Kasten, P., Beyen, I., Niemeyer, P., Luginbühl, R., Bohner, M., & Richter, W. (2008). Porosity and pore size of beta-tricalcium phosphate scaffold can influence protein production and osteogenic differentiation of human mesenchymal stem cells: an in vitro

and in vivo study. *Acta biomaterialia*, *4*(6), 1904–1915. https://doi.org/10.1016/j.actbio.2008.05.017

24. Liu, X., Holzwarth, J. M., & Ma, P. X. (2012). Functionalized synthetic biodegradable polymer scaffolds for tissue engineering. *Macromolecular bioscience*, *12*(7), 911–919. https://doi.org/10.1002/mabi.201100466

25. Kim, H. L., Jung, G. Y., Yoon, J. H., Han, J. S., Park, Y. J., Kim, D. G., Zhang, M., & Kim, D. J. (2015). Preparation and characterization of nano-sized hydroxyapatite/alginate/chitosan composite scaffolds for bone tissue engineering. *Materials science & engineering. C, Materials for biological applications*, *54*, 20–25. https://doi.org/10.1016/j.msec.2015.04.033

26. Goodarzi, H., Hashemi-Najafabadi, S., Baheiraei, N., & Bagheri, F. (2019). Preparation and Characterization of Nanocomposite Scaffolds (Collagen/β-TCP/SrO) for Bone Tissue Engineering. *Tissue engineering and regenerative medicine*, *16*(3), 237–251. https://doi.org/10.1007/s13770-019-00184-0

27. Wang, X., Lin, M., & Kang, Y. (2019). Engineering Porous β-Tricalcium Phosphate (β-TCP) Scaffolds with Multiple Channels to Promote Cell Migration, Proliferation, and Angiogenesis. *ACS applied materials & interfaces*, *11*(9), 9223–9232. https://doi.org/10.1021/acsami.8b22041

28. Hu, J., Smith, L. A., Feng, K., Liu, X., Sun, H., & Ma, P. X. (2010). Response of human embryonic stem cell-derived mesenchymal stem cells to osteogenic factors and architectures of materials during in vitro osteogenesis. *Tissue engineering. Part A*, *16*(11), 3507–3514. https://doi.org/10.1089/ten.TEA.2010.0097

29. Zhang, Z., Hu, J., & Ma, P. X. (2012). Nanofiber-based delivery of bioactive agents and stem cells to bone sites. *Advanced drug delivery reviews*, *64*(12), 1129–1141. https://doi.org/10.1016/j.addr.2012.04.008

30. Kokubo, T., & Takadama, H. (2006). How useful is SBF in predicting in vivo bone bioactivity?. *Biomaterials*, *27*(15), 2907–2915. https://doi.org/10.1016/j.biomaterials.2006.01.017

31. Murphy, W. L., Kohn, D. H., & Mooney, D. J. (2000). Growth of continuous bonelike mineral within porous poly(lactide-co-glycolide) scaffolds in vitro. *Journal of biomedical materials research*, *50*(1), 50–58. https://doi.org/10.1002/(sici)1097-4636(200004)50:1<50::aid-jbm8>3.0.co;2-f

32. Ślósarczyk, A., Paluszkiewicz, C., Gawlicki, M., & Paszkiewicz, Z. (1997). The FTIR spectroscopy and QXRD studies of calcium phosphate based materials produced from the powder precursors with different Ca/P ratios. *Ceramics International, 23*, 297-304.

33. Jeon, C., & Höll, W. H. (2003). Chemical modification of chitosan and equilibrium study for mercury ion removal. *Water research*, *37*(19), 4770–4780. https://doi.org/10.1016/S0043-1354(03)00431-7

34. Amaral, I. F., Granja, P. L., & Barbosa, M. A. (2005). Chemical modification of chitosan by phosphorylation: an XPS, FT-IR and SEM study. *Journal of biomaterials science. Polymer edition*, *16*(12), 1575–1593. https://doi.org/10.1163/156856205774576736

35. Yuan, Q., Shah, J., Hein, S., & Misra, R. D. (2010). Controlled and extended drug release behavior of chitosan-based nanoparticle carrier. *Acta biomaterialia*, *6*(3), 1140–1148. https://doi.org/10.1016/j.actbio.2009.08.027

36. Zeng, W., Huang, J., Hu, X., Xiao, W., Rong, M., Yuan, Z., & Luo, Z. (2011). Ionically cross-linked chitosan microspheres for controlled release of bioactive nerve growth factor. *International journal of pharmaceutics*, *421*(2), 283–290. https://doi.org/10.1016/j.ijpharm.2011.10.005

37. Thomas, M. S., Pillai, P. K., Faria, M., Cordeiro, N., Barud, H., Thomas, S., & Pothen, L. A. (2018). Electrospun polylactic acid-chitosan composite: a bio-based alternative for inorganic composites for advanced application. *Journal of Materials Science: Materials in Medicine*, *29*(9), 1-12.

38. Cardenas-Triviño, G., & Carrasco-Garcia, G. (2019). Chitosan composites prepared with hydroxyapatite and lactic acid as bone substitute. *Journal of the Chilean Chemical Society*, *64*(4), 4613-4618.

39. Danylchenko, S. M., Kalinkevich, O. V., & Pogorelov, M. V. (2009). Chitosan–hydroxyapatite composite biomaterials made by a one step co-precipitation method: preparation, characterization and in vivo tests.

40. Ahmed, G. M., Abouauf, E. A., AbuBakr, N., Dörfer, C. E., & El-Sayed, K. F. (2020). Tissue Engineering Approaches for Enamel, Dentin, and Pulp Regeneration: An Update. *Stem cells international*, *2020*, 5734539. https://doi.org/10.1155/2020/5734539

41. Bottino, M. C., Pankajakshan, D., & Nör, J. E. (2017). Advanced Scaffolds for Dental Pulp and Periodontal Regeneration. *Dental clinics of North America*, *61*(4), 689–711. https://doi.org/10.1016/j.cden.2017.06.009

42. Zhu, Y., Wan, Y., Zhang, J., Yin, D., & Cheng, W. (2014). Manufacture of layered collagen/chitosan-polycaprolactone scaffolds with biomimetic microarchitecture. *Colloids and Surfaces B: Biointerfaces*, *113*, 352-360.

43. Aranaz, I., Martínez-Campos, E., Moreno-Vicente, C., Civantos, A., García-Arguelles, S., & Del Monte, F. (2017). Macroporous Calcium Phosphate/Chitosan Composites Prepared via Unidirectional Ice Segregation and Subsequent Freeze-Drying. *Materials (Basel, Switzerland)*, *10*(5), 516. https://doi.org/10.3390/ma10050516

44. Chen, W., Zhou, H., Tang, M., Weir, M. D., Bao, C., & Xu, H. H. (2012). Gas-foaming calcium phosphate cement scaffold encapsulating human umbilical cord stem cells. *Tissue engineering. Part A*, *18*(7-8), 816–827. https://doi.org/10.1089/ten.TEA.2011.0267

45. Thein-Han, W., & Xu, H. H. (2013). Prevascularization of a gas-foaming macroporous calcium phosphate cement scaffold via coculture of human umbilical vein endothelial cells and osteoblasts. *Tissue engineering. Part A*, *19*(15-16), 1675–1685. https://doi.org/10.1089/ten.TEA.2012.0631

46. Chen, W., Thein-Han, W., Weir, M. D., Chen, Q., & Xu, H. H. (2014). Prevascularization of biofunctional calcium phosphate cement for dental and craniofacial repairs. *Dental materials : official publication of the Academy of Dental Materials*, *30*(5), 535–544. https://doi.org/10.1016/j.dental.2014.02.007

47. Dorozhkin S. V. (2012). Dissolution mechanism of calcium apatites in acids: A review of literature. *World journal of methodology*, *2*(1), 1–17. https://doi.org/10.5662/wjm.v2.i1.1

48. Shakir, M., Jolly, R., Khan, M. S., Iram, N. E., Sharma, T. K., & Al-Resayes, S. I. (2015). Synthesis and characterization of a nano-hydroxyapatite/chitosan/polyethylene glycol nanocomposite for bone tissue engineering. *Polymers for Advanced Technologies*, *26*(1), 41-48.

49. Kar, S., Kaur, T., & Thirugnanam, A. (2016). Microwave-assisted synthesis of porous chitosan–modified montmorillonite–hydroxyapatite composite scaffolds. *International journal of biological macromolecules*, *82*, 628-636.

50. Keikhaei, S., Mohammadalizadeh, Z., Karbasi, S., & Salimi A. (2019). Evaluation of the effects of β-tricalcium phosphate on physical, mechanical and biological properties of Poly (3-hydroxybutyrate)/chitosan electrospun scaffold for cartilage tissue engineering applications. *Materials Technology*, 34:10, 615-625. DOI: 10.1080/10667857.2019.1611053

51. Xin, R., Leng, Y., Chen, J., & Zhang, Q. (2005). A comparative study of calcium phosphate formation on bioceramics in vitro and in vivo. *Biomaterials*, *26*(33), 6477–6486. https://doi.org/10.1016/j.biomaterials.2005.04.028

52. Castro, N. J., Tan, W. N., Shen, C., & Zhang, L. G. (2016). Simulated Body Fluid Nucleation of Three-Dimensional Printed Elastomeric Scaffolds for Enhanced Osteogenesis. *Tissue engineering. Part A*, *22*(13-14), 940–948. https://doi.org/10.1089/ten.TEA.2016.0161

53. Shin, K., Acri, T., Geary, S., & Salem, A. K. (2017). Biomimetic Mineralization of Biomaterials Using Simulated Body Fluids for Bone Tissue Engineering and Regenerative Medicine. *Tissue engineering. Part A*, *23*(19-20), 1169–1180. https://doi.org/10.1089/ten.TEA.2016.0556

54. Yuan, X., Mak, A. F., & Li, J. (2001). Formation of bone-like apatite on poly(L-lactic acid) fibers by a biomimetic process. *Journal of biomedical materials research*, *57*(1), 140–150. https://doi.org/10.1002/1097-4636(200110)57:1<140::aid-jbm1153>3.0.co;2-g

55. An, S., Gao, Y., Ling, J., Wei, X., & Xiao, Y. (2012). Calcium ions promote osteogenic differentiation and mineralization of human dental pulp cells: implications for pulp capping materials. *Journal of materials science. Materials in medicine*, *23*(3), 789–795. https://doi.org/10.1007/s10856-011-4531-0

56. Gandolfi, M. G., Siboni, F., Botero, T., Bossù, M., Riccitiello, F., & Prati, C. (2015). Calcium silicate and calcium hydroxide materials for pulp capping: biointeractivity, porosity, solubility and bioactivity of current formulations. *Journal of applied biomaterials & functional materials*, *13*(1), 43–60. https://doi.org/10.5301/jabfm.5000201

57. Kuzmenka, D., Sewohl, C., König, A., Flath, T., Hahnel, S., Schulze, F. P., Hacker, M. C., & Schulz-Siegmund, M. (2020). Sustained Calcium(II)-Release to Impart Bioactivity in Hybrid Glass Scaffolds for Bone Tissue Engineering. *Pharmaceutics*, *12*(12), 1192. https://doi.org/10.3390/pharmaceutics12121192

58. Farhadian, N, Godiny, M., Moradi, S., Azandaryani, A. H., Shahlaei, M. (2018). Chitosan/gelatin as a new nano-carrier system for calcium hydroxide delivery in endodontic applications: Development, characterization and process optimization. *Materials Science and Engineering: C*, 92, 540-546. https://doi.org/10.1016/j.msec.2018.07.002.

59. Flores-Arriaga, J. C., Pozos-Guillén, A. J., González-Ortega, O., Escobar-García, D. M., Masuoka-Ito, D., Del Campo-Téllez, B., & Cerda-Cristerna, B. I. (2019). Calcium sustained release, pH changes and cell viability induced by chitosan-based pastes for apexification. *Odontology*, *107*(2), 223–230. https://doi.org/10.1007/s10266-018-0389-7

60. Boone, P. S., Zimmerman, M. C., Gutteling, E., Lee, C. K., Parsons, J. R., & Langrana, N. (1989). Bone attachment to hydroxyapatite coated polymers. Journal of biomedical materials research, 23(A2 Suppl), 183–199.

61. Al-Munajjed, A. A., Plunkett, N. A., Gleeson, J. P., Weber, T., Jungreuthmayer, C., Levingstone, T., Hammer, J., & O'Brien, F. J. (2009). Development of a biomimetic collagen-hydroxyapatite scaffold for bone tissue engineering using a SBF immersion technique. *Journal of biomedical materials research. Part B, Applied biomaterials*, *90*(2), 584–591. https://doi.org/10.1002/jbm.b.31320

Figure Captions

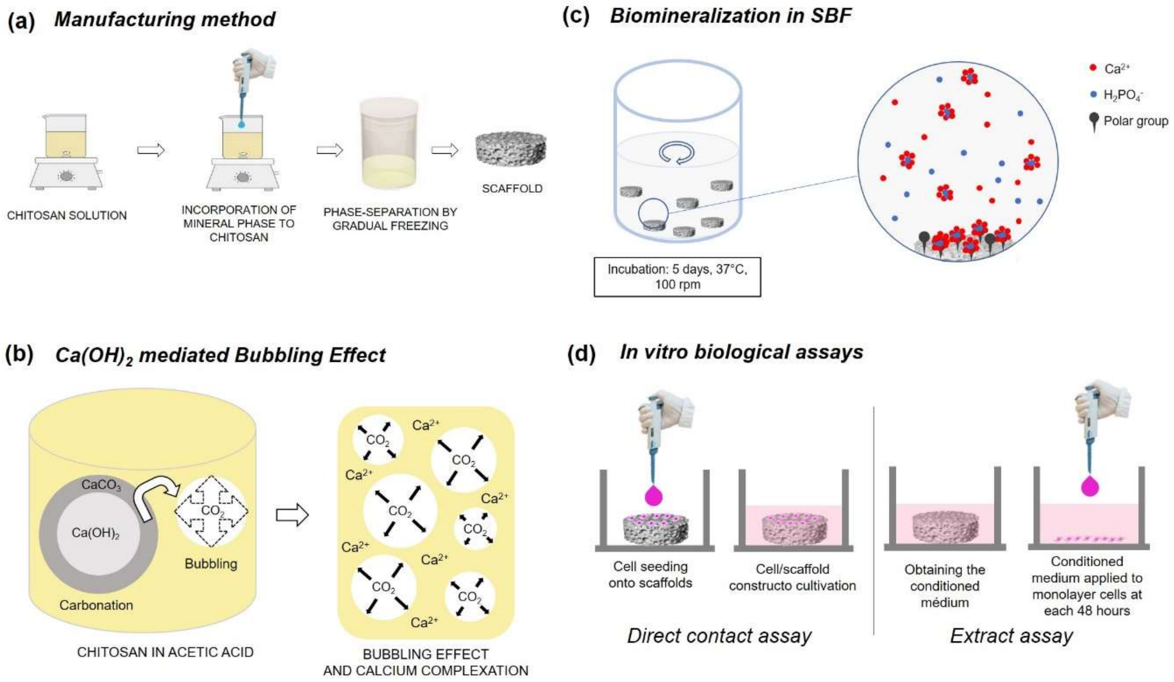
(a) Manufacturing method
CHITOSAN SOLUTION
INCORPORATION OF MINERAL PHASE TO CHITOSAN
PHASE-SEPARATION BY GRADUAL FREEZING
SCAFFOLD
(c) Biomineralization in SBF
Incubation: 5 days, 37°C, 100 rpm
Ca2+
H2PO4-
Polar group
(b) Ca(OH)2 mediated Bubbling Effect
CaCO3
Ca(OH)2
CO2
Bubbling
Carbonation
CHITOSAN IN ACETIC ACID
Ca2+
BUBBLING EFFECT AND CALCIUM COMPLEXATION
(d) In vitro biological assays
Cell seeding onto scaffolds
Cell/scaffold constructo cultivation
Obtaining the conditioned médium
Conditioned medium applied to monolayer cells at each 48 hours
Direct contact assay
Extract assay

FIGURE 1 Representative schematics of manufacturing method (a), $Ca(OH)_2$ mediated Bubbling Effect (b), biomineralization in SBF (c) and in vitro biological methods (d).

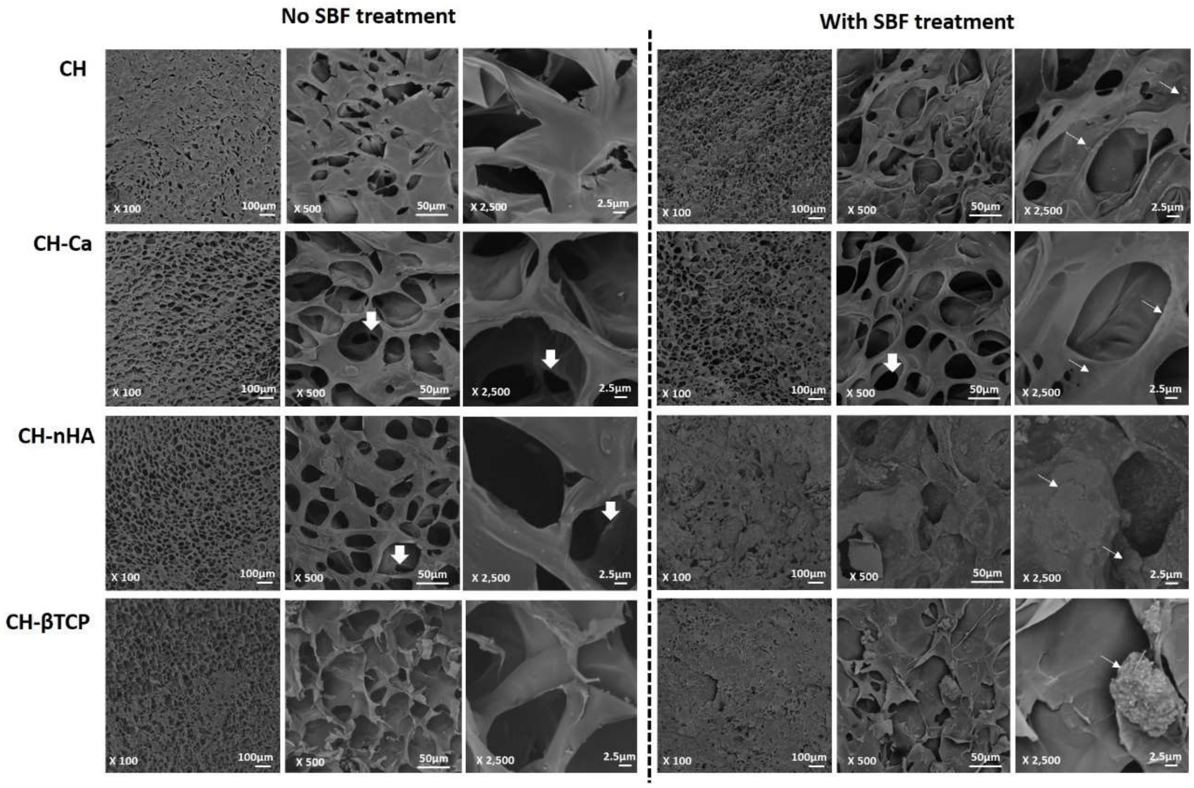
No SBF treatment
With SBF treatment
CH
CH-Ca
CH-nHA
CH-βTCP
X 100
100µm
X 500
50µm
X 2,500
2.5µm

FIGURE 2 Scaffold architecture. SEM images of the surfaces of scaffolds subjected or not to SBF treatment. Magnifications of 100x, 500x, and 2500x. Note the round and well-organized pore network on CH-Ca and CH-nHA scaffolds not treated with SBF. Pore interconnectivity is indicated by large white arrows. CH-Ca treated with SBF maintained this porous network. Slight and sparse deposition of mineral-like structure is seen in SBF-treated CH and CH-Ca scaffolds (arrows). Mineral deposits can be easily detected on CH-nHA and CH-βTCP scaffolds treated with SBF (arrows), along with a disorganized and low porous architecture

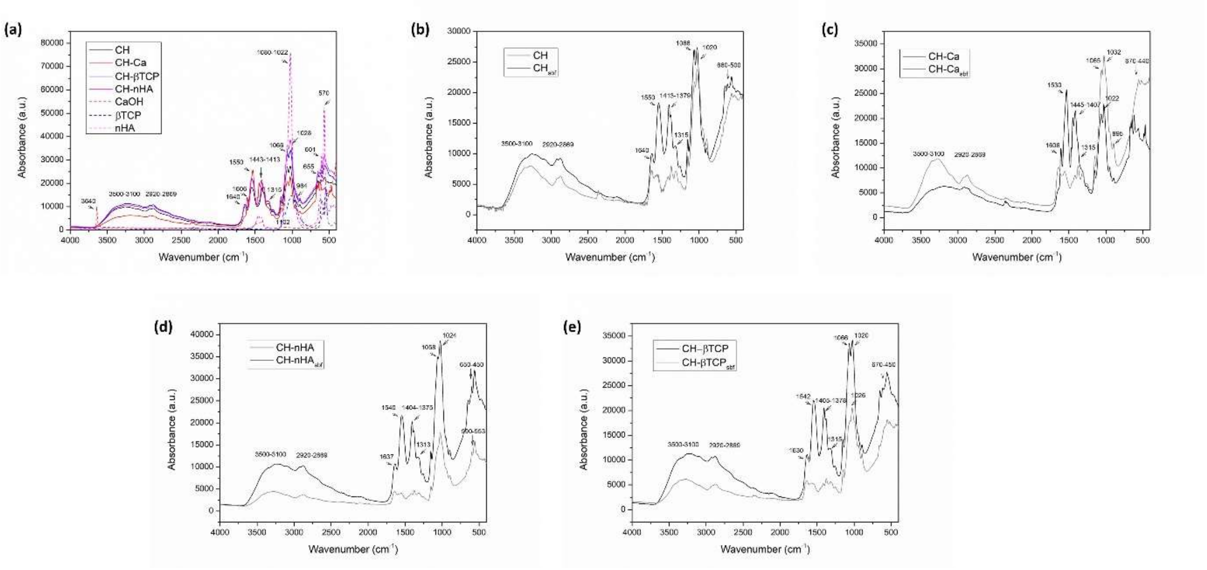

FIGURE 3 Chemical composition. Comparison of FTIR spectra after addition of mineral phases (a) and before and after incubation in SBF: CH and CH$_{SBF}$ (b); CH-Ca and CH-Ca$_{SBF}$ (c); CH-nHA and CH-nHA$_{SBF}$ (d); CH-βTCP and CH-βTCP$_{SBF}$ (e).

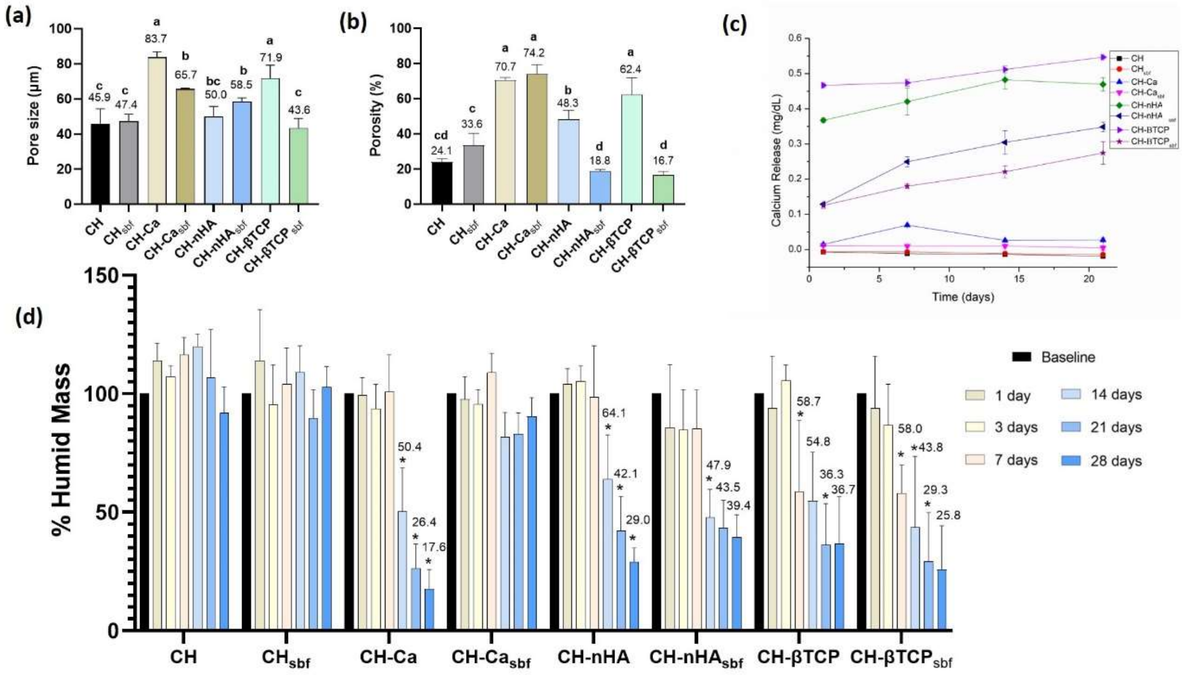

FIGURE 4 Physical characterization. Bar graph representing the mean values of pore size (a) and porosity degree (b). Numbers are mean values. Different letters indicate statistically significant differences among the groups (one-way ANOVA/Tukey´s test; *p* < .05). (c) Graph representative of mean and standard deviation values of cumulative calcium release (mg/dL) at 1, 7, 14, and 21 days. (d) Bar graph representing the mean humid mass % values. *Statistically significant difference from the immediately preceding analysis period (one-way ANOVA/Dunnett's test; *p* < .05)

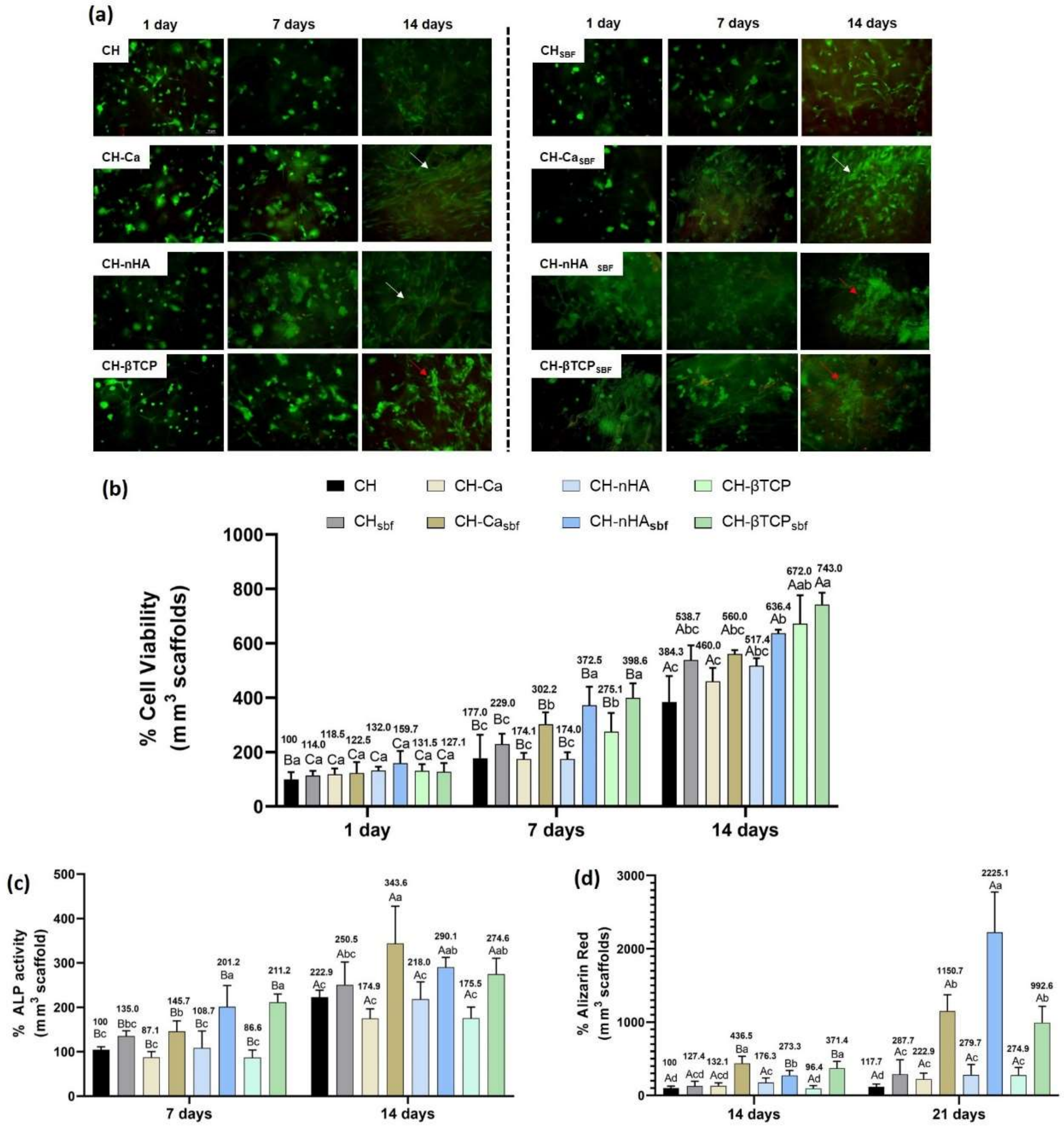

FIGURE 5 Direct contact assay. (a) Representative images of the Live/Dead assay. Green, viable cells; red, dead cells. 20x magnification. White arrows indicate cells with stretched cytoplasm. Red arrows indicate cells in agglomerates. (b, c, d) Alamar Blue assay, ALP activity, and Alizarin red assays, respectively. Bar graph representing the mean values (numbers). Capital letters allow for comparisons among the time-points for each experimental group. Lower-case letters allow for comparisons between and among experimental groups within each time-point. Different letters indicate statistically significant differences (RM two-way ANOVA/Tukey's test; $p < .05$)

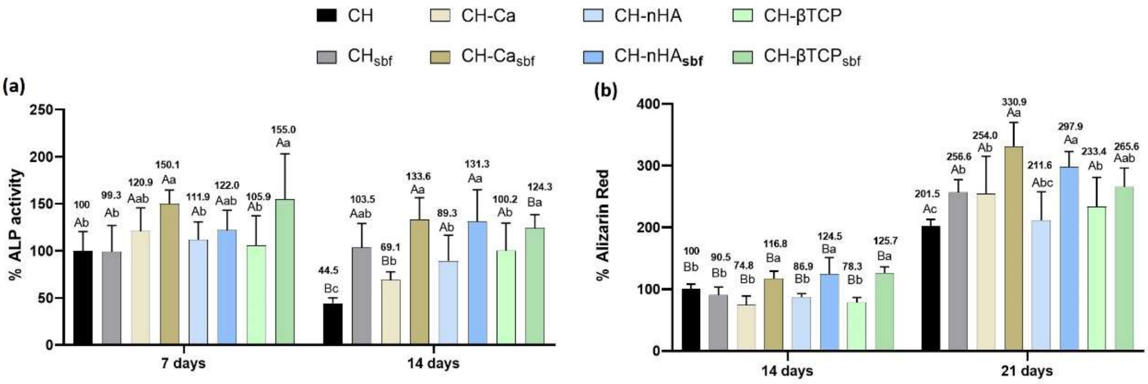

FIGURE 6 Conditioned medium assay. (a, b) ALP activity and Alizarin red assays, respectively. Bar graph representing the mean values (numbers). Capital letters allow for comparisons between the analysis periods for each experimental group. Lower-case letters allow for comparisons between and among experimental groups within each period of analysis. Different letters indicate statistically significant differences (two-way ANOVA/Tukey's test; $p < .05$)

3 FINAL CONSIDERATIONS

3 FINAL CONSIDERATIONS

Currently, researchers seek biofabrication strategies to develop biomaterials capable of stimulating pulp cells to differentiate and produce a mineralized barrier, for application in Vital Pulp Therapy (VPT). $Ca(OH)_2$ is one of the main materials used for this purpose in dental practice, due to its low cost and antimicrobial potential. Among its main disadvantages, we can mention coagulation necrosis and inflammatory reactions on pulp tissue following its application, which precedes the deposition of mineralized matrix. The ideal material for application in VPT would be one capable of stimulating mineralized barrier deposition, but without this deleterious effect. Calcium-phosphate mineral phases, such as βTCP and HA, have been studied as biomaterials for bone and dentin tissue engineering because they are biocompatible, bioactive, and osteoconductive. With this in mind, we synthesized chitosan scaffolds containing $Ca(OH)_2$, nHA, and βTCP, and coated them with hydroxyapatite through incubation in SBF, aiming at dentin repair. The surface morphology, pore structure, chemical composition, calcium-release capacity, and degree of degradation of the scaffolds were investigated, in addition to their biological effects on dental pulp cells.

The fabrication process presented in this study represents alternatives to the technique previously developed by our group, in which $Ca(OH)_2$ effectively acted as a CO_2 releaser and Ca^{2+} donor during a defined phase-separation technique, and in which highly porous chitosan scaffolds containing calcium complexed to their structure were created (CH-Ca). An outstanding feature of this technique is the well-organized and interconnected round porous architecture, which allows cells to infiltrate its porous network easily, an essential feature for cell-homing applications. Here, we also tested a calcium-phosphate mineral phase with recognized bioactive potential for bone regeneration. Only nHA was capable of promoting a similar bubbling effect on a chitosan scaffold such as $Ca(OH)_2$. Nevertheless, the pore size and porosity degree were significantly lower than those of our traditional CH-Ca scaffold. Another important result of this study is that all three mineral phases tested presented similar bioactive potential for human dental pulp cells, which means that a low-cost formulation based on $Ca(OH)_2$ features the same bioactive potential as nHA and βTCP, which are highly expensive biomaterials.

With the aim of improved bioactivity, the formulated scaffolds were subjected to biomineralization in SBF, with the goal of depositing a layer of hydroxyapatite onto the scaffold structure. This process was effective, since bioactivity was intensely improved for all tested formulations. Nevertheless, only CH-Ca retained the macro-porous architecture following this process. Therefore, once more, this low-cost formulation seems to be an interesting alternative to the creation of highly bioactive scaffolds for dentin regeneration, providing an interconnected porous structure to allow for resident cell infiltration along with the establishment of an internal capillary network. The results presented in this work are proof-of-principle that the fabrication process developed by our group presents significant potential to create biomimetic scaffolds for dentin tissue engineering. Nevertheless, further studies are necessary to prove its applicability as a cell-free platform for dentin regeneration, in in vivo models prior to application in human subjects.

REFERENCES

REFERENCES

1. Gupte MJ, Ma PX. Nanofibrous scaffolds for dental and craniofacial applications. J Dent Res. 2012 Mar;91(3):227-34.

2. Rosa V, Della Bona A, Cavalcanti BN, Nör JE. Tissue engineering: from research to dental clinics. Dent Mater. 2012 Apr;28(4):341-8.

3. Costello BJ, Kumta P, Sfeir CS. Regenerative Technologies for Craniomaxillofacial Surgery. J Oral Maxillofac Surg. 2015 Dec;73(12 Suppl):S116-25. doi: 10.1016/j.joms.2015.04.036. PMID: 26608139.

4. Tollemar V, Collier ZJ, Mohammed MK, Lee MJ, Ameer GA, Reid RR. Stem cells, growth factors and scaffolds in craniofacial regenerative medicine. Genes Dis. 2016 Mar;3(1):56-71. doi: 10.1016/j.gendis.2015.09.004. Epub 2015 Oct 17. PMID: 27239485; PMCID: PMC4880030.

5. BaoLin G, Ma PX. Synthetic biodegradable functional polymers for tissue engineering: a brief review. Sci China Chem. 2014 Apr 1;57(4):490-500. doi: 10.1007/s11426-014-5086-y. PMID: 25729390; PMCID: PMC4341840.

6. Piva E, Silva AF, Nör JE. Functionalized scaffolds to control dental pulp stem cell fate. J Endod. 2014 Apr;40(4 Suppl):S33-40.

7. Galler KM, Eidt A, Schmalz G. Cell-free approaches for dental pulp tissue engineering. J Endod. 2014 Apr;40(4 Suppl):S41-5.

8. Soares DG, Zhang Z, Mohamed F, Eyster TW, de Souza Costa CA, Ma PX. Simvastatin and nanofibrous poly(l-lactic acid) scaffolds to promote the odontogenic potential of dental pulp cells in an inflammatory environment. Acta Biomater. 2018 Mar 1;68:190-203.

9. Zhang R, Ma PX. Biomimetic polymer/apatite composite scaffolds for mineralized tissue engineering. Macromol Biosci. 2004 Feb 20;4(2):100-11.

10. Wei G, Ma PX. Macroporous and nanofibrous polymer scaffolds and polymer/bone-like apatite composite scaffolds generated by sugar spheres. J Biomed Mater Res A. 2006 Aug;78(2):306-15.

11. Murray PE. Constructs and scaffolds employed to regenerate dental tissue. Dent Clin North Am. 2012 Jul;56(3):577-88.

12. Sergeeva, Alena S., Dmitry A. Gorin, and Dmitry V. Volodkin. "In-Situ Assembly of Ca–Alginate Gels with Controlled Pore Loading/Release Capability." *Langmuir* 31.39 (2015): 10813-10821.

13. Kim HL, Jung GY, Yoon JH, Han JS, Park YJ, Kim DG, Zhang M, Kim DJ. Preparation and characterization of nano-sized hydroxyapatite/alginate/chitosan composite scaffolds for bone tissue engineering. Mater Sci Eng C Mater Biol Appl. 2015 Sep;54:20-5.

14. Saravanan S, Leena RS, Selvamurugan N. Chitosan based biocomposite scaffolds for bone tissue engineering. Int J Biol Macromol. 2016 Dec;93(Pt B):1354-1365.

15. Flores-Arriaga JC, Pozos-Guillén AJ, González-Ortega O, Escobar-García DM, Masuoka-Ito D, Del Campo-Téllez BIM, Cerda-Cristerna BI. Calcium sustained release, pH changes and cell viability induced by chitosan-based pastes for apexification. Odontology. 2019 Apr;107(2):223-230. doi: 10.1007/s10266-018-0389-7. Epub 2018 Sep 18. PMID: 30229345.

16. Madihally SV, Matthew HW. Porous chitosan scaffolds for tissue engineering. Biomaterials. 1999 Jun;20(12):1133-42. doi: 10.1016/s0142-9612(99)00011-3. PMID: 10382829.

17. Li F, Liu X, Zhao S, Wu H, Xu HH. Porous chitosan bilayer membrane containing TGF-β1 loaded microspheres for pulp capping and reparative dentin formation in a dog model. Dent Mater. 2014 Feb;30(2):172-81.

18. Soares DG, Anovazzi G, Bordini EAF, Zuta UO, Silva Leite MLA, Basso FG, Hebling J, de Souza Costa CA. Biological Analysis of Simvastatin-releasing Chitosan Scaffold as a Cell-free System for Pulp-dentin Regeneration. J Endod. 2018 Jun;44(6):971-976.e1.

19. Pestov A, Bratskaya S. Chitosan and Its Derivatives as Highly Efficient Polymer Ligands. Molecules. 2016 Mar 11;21(3):330.

20. Zhang Z, Hu J, Ma PX. Nanofiber-based delivery of bioactive agents and stem cells to bone sites. Adv Drug Deliv Rev. 2012 Sep;64(12):1129-41.

21. Soares DG, Bordini EAF, Cassiano FB, Bronze-Uhle ES, Pacheco LE, Zabeo G, Hebling J, Lisboa-Filho PN, Bottino MC, de Souza Costa CA. Characterization of novel calcium hydroxide-mediated highly porous chitosan-calcium scaffolds for potential application in dentin tissue engineering. J Biomed Mater Res B Appl Biomater. 2020 Aug;108(6):2546-2559. doi: 10.1002/jbm.b.34586. Epub 2020 Feb 15. PMID: 32061059.

22. Hu J, Smith LA, Feng K, Liu X, Sun H, Ma PX. Response of human embryonic stem cell-derived mesenchymal stem cells to osteogenic factors and architectures of materials during in vitro osteogenesis. Tissue Eng Part A. 2010 Nov;16(11):3507-14.

23. Liu X, Holzwarth JM, Ma PX. Functionalized synthetic biodegradable polymer scaffolds for tissue engineering. Macromol Biosci. 2012 Jul;12(7):911-9.

24. Soares DG, Rosseto HL, Basso FG, Scheffel DS, Hebling J, Costa CA. Chitosan-collagen biomembrane embedded with calcium-aluminate enhances dentinogenic potential of pulp cells. Braz Oral Res. 2016;30(1):e54.

25. Soares DG, Rosseto HL, Scheffel DS, Basso FG, Huck C, Hebling J, de Souza Costa CA. Odontogenic differentiation potential of human dental pulp cells cultured on a calcium-aluminate enriched chitosan-collagen scaffold. Clin Oral Investig. 2017 Dec;21(9):2827-2839.

26. Bordini EAF, Cassiano FB, Silva ISP, Usberti FR, Anovazzi G, Pacheco LE, Pansani TN, Leite ML, Hebling J, de Souza Costa CA, Soares DG. Synergistic potential of 1α,25-dihydroxyvitamin D3 and calcium-aluminate-chitosan scaffolds with dental pulp cells. Clin Oral Investig. 2020 Feb;24(2):663-674.

27. Guastaldi AC, Aparecida AH. Fosfatos de cálcio de interesse biológico: importância como biomateriais, propriedades e métodos de obtenção de recobrimentos. Quim. Nova. 2010;33(6), 1352-1358.

28. Kasten P, Beyen I, Niemeyer P, Luginbühl R, Bohner M, Richter W. Porosity and pore size of beta-tricalcium phosphate scaffold can influence protein production and osteogenic differentiation of human mesenchymal stem cells: an in vitro and in vivo study. Acta Biomater. 2008 Nov;4(6):1904-15.

29. AbdulQader ST, Kannan TP, Rahman IA, Ismail H, Mahmood Z. Effect of different calcium phosphate scaffold ratios on odontogenic differentiation of human dental pulp cells. Mater Sci Eng C Mater Biol Appl. 2015 Apr;49:225-233. doi: 10.1016/j.msec.2014.12.070. Epub 2014 Dec 20. PMID: 25686943.

30. Goodarzi H, Hashemi-Najafabadi S, Baheiraei N, Bagheri F. Preparation and Characterization of Nanocomposite Scaffolds (Collagen/β-TCP/SrO) for Bone Tissue Engineering. Tissue Eng Regen Med. 2019 Mar 21;16(3):237-251.

31. Wang X, Lin M, Kang Y. Engineering Porous β-Tricalcium Phosphate (β-TCP) Scaffolds with Multiple Channels to Promote Cell Migration, Proliferation, and Angiogenesis. ACS Appl Mater Interfaces. 2019 Mar 6;11(9):9223-9232.

32. Guerrero-Gironés J, Alcaina-Lorente A, Ortiz-Ruiz C, Ortiz-Ruiz E, Pecci-Lloret MP, Ortiz-Ruiz AJ, Rodríguez-Lozano FJ, Pecci-Lloret MR. Biocompatibility of a HA/β-TCP/C Scaffold as a Pulp-Capping Agent for Vital Pulp Treatment: An In Vivo Study in Rat Molars. Int J Environ Res Public Health. 2021 Apr 8;18(8):3936.

33. Kokubo T, Takadama H. How useful is SBF in predicting in vivo bone bioactivity? Biomaterials. 2006 May;27(15):2907-15. doi: 10.1016/j.biomaterials.2006.01.017. Epub 2006 Jan 31. PMID: 16448693.

34. Murphy WL, Kohn DH, Mooney DJ. Growth of continuous bonelike mineral within porous poly(lactide-co-glycolide) scaffolds in vitro. J Biomed Mater Res. 2000 Apr;50(1):50-8. doi: 10.1002/(sici)1097-4636(200004)50:1<50::aid-jbm8>3.0.co;2-f. PMID: 10644963.

APPENDIX

APÊNDICE A - DECLARAÇÃO DE USO EXCLUSIVO DE ARTIGO EM DISSERTAÇÃO/TESE

DECLARATION OF EXCLUSIVE USE OF THE ARTICLE IN DISSERTATION/THESIS

We hereby declare that we are aware of the article **Mineral-induced bubbling effect and biomineralization as strategies to create highly porous and bioactive scaffolds for dentin tissue engineering** will be included in Dissertation of the student Camila Correa da Silva Braga de Melo was not used and may not be used in other works of Graduate Programs at the Bauru School of Dentistry, University of São Paulo.

Bauru, 08 de novembro de 2021.

Camila Correa da Silva Braga de Melo
Author

Camila Correa S. B. de Melo
Signature

Diana Gabriela Soares dos Passos
Author

Signature